

AD-753 843

PHYSIOLOGICAL EFFECTS OF LOW VENTILA-  
TION RATES, HIGH TEMPERATURES AND HIGH  
HUMIDITIES

Richard K. Peifley, et al

Santa Clara University

Prepared for:

Defense Civil Preparedness Agency

June 1972

DISTRIBUTED BY:

**NTIS**

National Technical Information Service  
U. S. DEPARTMENT OF COMMERCE  
5285 Port Royal Road, Springfield Va. 22151

**PHYSIOLOGICAL EFFECTS OF LOW VENTILATION  
RATES, HIGH TEMPERATURES & HIGH HUMIDITIES**

**FINAL REPORT**

Defense Civil Preparedness Agency  
Department of Defense

Contract No. DAHC-20-69-C-0128  
Work Unit No. 1224C

AD753843

NATIONAL TECHNICAL  
INFORMATION SERVICE

ME-72-1

*The University of Santa Clara • California*



THIS DOCUMENT HAS BEEN APPROVED FOR PUBLIC RELEASE AND SALE; ITS DISTRIBUTION IS UNLIMITED

PHYSIOLOGICAL EFFECTS OF LOW VENTILATION  
RATES, HIGH TEMPERATURES AND HIGH HUMIDITIES

FINAL REPORT

by

Richard K. Pefley  
Joseph F. Abel  
John S. Dutton

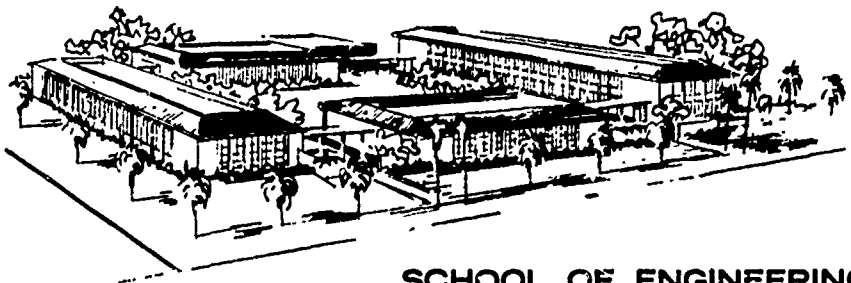
June 1972

Approved for Public Release; Distribution Unlimited  
for

Defense Civil Preparedness Agency  
Department of Defense  
Washington, D.C. 20301

Contract No. DAHC-20-69-C-0128  
Work Unit No. 1224C

DCPA REVIEW NOTICE: This report has been reviewed in the Defense Civil Preparedness Agency and approved for publication. Approval does not signify that the contents necessarily reflect the views and policies of the Defense Civil Preparedness Agency.



**SCHOOL OF ENGINEERING**

**ENGINEERING AND APPLIED SCIENCE RESEARCH**

**UNIVERSITY OF SANTA CLARA**

**SANTA CLARA, CALIFORNIA    AREA CODE 408-984-4325**

## ABSTRACT

Through the use of a predictive model and experimentation in a calorimeter, the temperatures and humidities which represent equal comfort states to the human for minimal ventilation rates in a neutral thermal radiation environment are established. This is accomplished by establishing from experimental data a relationship between the subject's skin temperature and the per cent of sweat glands that are activated. Points on the resulting curve are defined as values on the Physiological Thermal Index. They are used in conjunction with experimentally obtained heat and mass transfer coefficients to place lines on the psychrometric chart which represent constant values of this index. The effects of variations in air flow rate, and metabolic output, are presented. The predicted results are also compared with experimental evidence from the calorimeter and with the effective temperature values from the literature. The evidence to date indicates that the predictive model is sound and that the Physiological Thermal Index affords a new and clearer way to view the interaction between man and his thermal environment.

A predictive model for determining human thermal response to transient radiant flux of the type associated with building fires in spaces adjacent to survival shelters is also present. It is built upon the concepts previously discussed and includes the thermal capacitance of the test subject. Depending upon the onset rate of flux generation, it is shown that the skin temperature can be driven above body core temperature. A plan for experimentally verifying the results from the predictive model using the human calorimeter is discussed.

## INDEX

	<u>Page</u>
I. INTRODUCTION	1
Previous Work Summary	1
Present Program Objectives	2
Physical Basis for the Predictive Model	3
Experimental Apparatus	3
Instrumentation and Test Procedure	5
Report Presentation Format	6
II. ENERGY BALANCE AND TRANSPORT RATE EQUATIONS	8
Heat and Mass Transfer Rate Equations	8
Natural Motion Limit	11
Evaluation of Convective Heat Transfer Coefficient	11
Evaluation of Convective Mass Transfer Coefficient and Per Cent Active Sweat Glands	11
III. THE RELATIONSHIP BETWEEN $(x - T_s)$ AND STATES OF EQUAL COMFORT	15
Interpretation of $(x - T_s)$ Relationship	16
Subdivision of the $(x - T_s)$ Relationship	16
(1) Insensible or Passive Sweating Region	16
(2) Modulated Active or Sensible Sweating Region	17
(3) Heat Stroke Region	17
Physiological Thermal Index	18
IV. THE LOCI OF PTI VALUES ON THE PSYCHROMETRIC CHART	23
Derivation of Psychrometric Equations Using PTI Values	23
Generation of Lines for PTI Constant Values	26
Characteristics of Predicted PTI Lines	26
Comparison Between Yaglou's Values and Predicted PTI Lines for Adult Males	29
Establishment of Thermal Comfort Zones on $(x - T_s)$ Relationship and Interpretation on the Psychro- metric Chart	32
PTI Lines Compared with Other Evidence from the Literature	33
Subjective Experimental Response Compared to the New PTI Lines	36

	<u>Page</u>
Plausible Conclusions	39
Predicted PTI Lines of Adult Males Compared with General Population	39
Predicted PTI Lines for Subjects in Environments of High Air Velocities and Radiant Heat Exchange	42
Non-Isostate Process Lines	44
V. RESPONSE TO A TRANSIENT THERMAL FLUX	48
Review of Literature Predictive Models	48
Discussion of the Transient Thermal Flux	51
Predictive Model Problem Statement, Assumption, and Thermal Circuit Schematic	51
Derivation of Thermal Response Equations	55
Method of Solution	56
Interpretation of Results	56
VI. SUMMARY, CONCLUSION AND RECOMMENDATIONS FOR FOLLOW-ON ACTIVITIES	60
Project Summary and Conclusions	60
Recommendations for Follow-on Activities	62
APPENDICES	
1. Skin Temperature Apparatus	64
2. Logarithmic Mean Average	67
3. Symbols Used in the Program	70
Program Statements	71
REFERENCES	73

## LIST OF FIGURES

	<u>Page</u>
Fig. 1 Monoman Calorimeter	4
Fig. 2 Ave. Mass Transfer Coef. Vs. Skin Temperature	13
Fig. 3 Body Wetness Fraction Vs. Skin Temperature	14
Fig. 4 Physiological Thermal Index (PTI) Superimposed on $x - T_s$ Relationship	22
Fig. 5 Predicted Nude PTI Lines for General Population Using $x - T_s$ Curve	27
Fig. 6 Predicted Nude PTI Lines for Adult Males Using $x - T_s$ Curve	28
Fig. 7 Variation of $x$ with C.P. Yaglou ET Lines for Nude General Population and Very Low Flow Rate	31
Fig. 8 Thermal Comfort Zones on $(x - T_s)$ Curve	34
Fig. 9 Comfort Zones for Sedentary Semi-Nude Adult Males Under Very Low Air Flow Rates	35
Fig. 10 Predicted Nude PTI Lines for Adult Males Compared with Gagge and KSU	37
Fig. 11 Predicted PTI Lines of Nude Adult Males Compared with General Population	41
Fig. 12 Environmental Effects on Natural Motion Limit PTI Line Locations	43
Fig. 13 Non-Isostate Process Lines Versus CFM for Constant Average PTI of 5.0 (General Population)	45
Fig. 14 Non-Isostate Process Lines Versus CFM for Constant Average PTI of -1.8 (General Population)	46
Fig. 15 Apparent Body Conductive Resistance Versus Skin Temperature	53
Fig. 16 Thermal Circuit Representing Subject Exposed to Proposed Transient Thermal Environment	54
Fig. 17 Human Temperature Response to Radiation Flux Simulating a Fire Above the Ceiling	57

## I. INTRODUCTION

### Previous Work Summary

This investigation was undertaken as a continuation of the Monoman Calorimeter Project [1]\*, which is a study of the human thermal reaction to simulated crowded conditions and low ventilation rates. For the past five years tests have been conducted on a sample population of adult males, females and children under high dry bulb temperatures, high humidities and very low air flow rates. Most of the data generated was along 82, 85, and 90°F effective temperature lines. The previously reported work primarily examined metabolic rates and the process lines generated by test subjects in this severe thermal environment. Based on the experimental evidence it was shown that a standard population sample under sedentary conditions generates an average metabolic output of 275 Btu/hr. This indicated that the 400 Btu/hr commonly used in planning has a considerable safety margin unless the shelterees are all young men who indeed do have a typical metabolic rate of 400 Btu/hr. The concepts of non-isostate and isostate environments were established as the extreme process limits between which an actual shelter process must lie.

During this earlier work part of the investigation was to evaluate the effective temperature lines, developed by F. C. Houghton and C. P. Yaglou [2], from subjective response of the test subjects. The question being whether the effective temperature concept would truly represent equal comfort states for minimal air circulation. Many laboratories and field workers [3]

---

\*The numbers in brackets designate references listed in the bibliography.



have found that this index overestimates the influence of humidity on sensations of warmth and comfort at ordinary temperatures, and underestimates the effect in very high temperatures. The effective temperature lines indicate a person's feeling of warmth immediately after entering a conditioned space. Overestimation of the humidity effect in the absence of sweat gland activity (referred to here as insensible evaporation) is explained by adsorption and desorption phenomena and by failure to take adaptation into account [4]. Several studies have been done to improve the ET lines. Hardy and DeBois [5], and Gagge, et al., [6] have found a close relationship between mean skin temperature and comfort in air conditions that lie below the zone of active evaporative cooling. C. P. Yaglou has found mean skin temperature is a fairly sensitive index of warmth in temperatures under 82°F, or when persons are not actively sweating. He suggested that the mean skin temperature be taken as an index of comfort when there is no active evaporative cooling. In the zone of active evaporation cooling the skin temperature rises very slowly while the evaporative heat loss rises very sharply [7].

Many experiments have been made to study the relation between total evaporative heat loss and operative temperature when radiant, convective and evaporative heat exchanges are present. C. E. Winslow, L. P. Herrington and A. P. Gagge studied the relation between total evaporative heat loss and mean skin temperature [7].

#### Present Program Objectives

- (a) To establish a physical basis for the prediction of lines of equal comfort for semi-nude persons in equilibrium with

environmental conditions of very low air flow rates and within the range wherein the human body can maintain a thermal regulatory control.

- (b) To use this as a basis for predicting lines of equal comfort on the psychrometric chart.
- (c) To compare test subject response with the predictive model by use of the calorimeter.
- (d) To extend the predictive model to include transient behavior associated with a thermal radiation pulse.

#### Physical Basis for the Predictive Model

The physical basis for the predictive model lies in three relationships:

- (a) The relationship between the skin temperature and percentage of the sweat glands that are actively sweating.
- (b) Energy balance equations between the human body and the environment.
- (c) Heat and mass transport rate equations between the person and his surroundings.

#### Experimental Apparatus

The apparatus used to gather the experimental data is the monoman calorimeter, shown in Fig. 1, which was designed originally to simulate the environment of an overcrowded survival shelter under the condition of very low air flow rates. The main components of the calorimeter are the adiabatic test cell in which the test subject is encapsulated and the ventilation system. The test cell is a fabricated bag made of polyethylene sheet and plastic tape. The bag is lined on the inside with aluminized mylar while

MONOMAN CALORIMETER<sup>4</sup>  
SCALE 3/4" = 1'

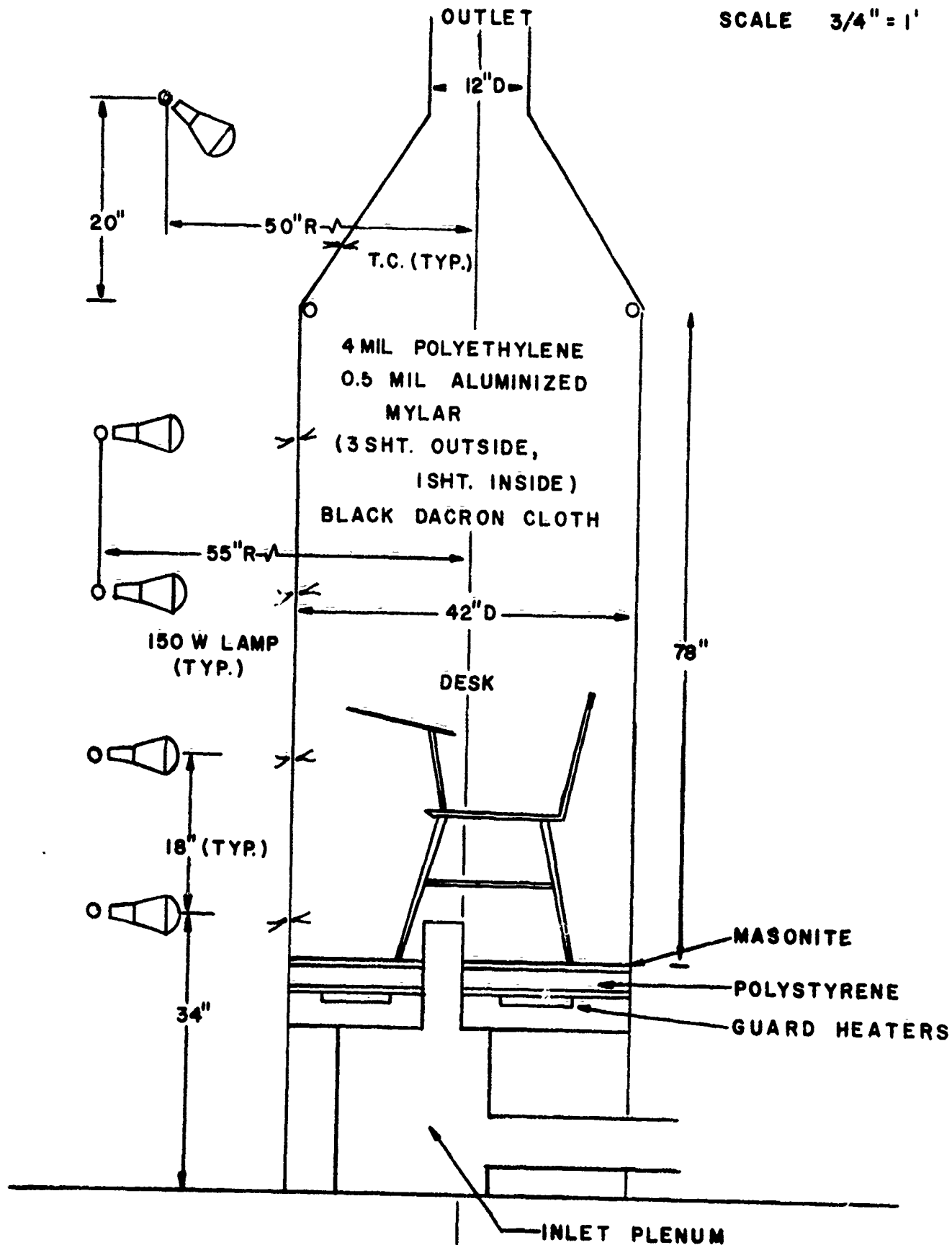


FIGURE 1

it is covered on the outside with several sheets of aluminized mylar separated by a sheet of air cap. The net radiative heat exchange between the calorimeter and the test subject is negligible because of the reflective walls of the calorimeter which simulates being surrounded by others. The bag has excellent thermal response characteristics and high thermal resistance. Adiabatic conditions are maintained by automatically adjusting the intensity of five rings of lamps that radiate heat to the calorimeter wall. Air supply for the calorimeter with desired quantity, temperature and humidity is from an air-conditioning apparatus. For more details see reference [1].

#### Instrumentation and Test Procedure

Measured quantities of primary interest are wet and dry bulb temperatures at inlet and exhaust, air flow rate, and temperature gradients across the walls and base to insure adiabatic condition. Thermocouples are used to measure wet and dry bulb temperatures while a positive displacement flow meter and stop watch are used to measure the air flow rate.

Physiological measurements of primary interest are pulse, oral temperature, and skin temperature. The skin temperature is taken as the weighted average of readings of nine thermistors located at different points on the body surface. As the skin temperature harness was developed as part of the current project, it is discussed in detail in Appendix 1.

After the system is brought to the desired condition, the person to be tested is secured in the calorimeter. The equilibrium condition of the person and the calorimeter is reached by

automatically adjusting the heating lamps until the calorimeter walls are adiabatic while holding air inlet temperature, humidity and flow rate constant. Data is taken after observing constant conditions of the calorimeter and the subject.

An analytical attempt to correlate the convective coefficients with low air velocities and with the free convection parameters [8] failed because the random motions of the test subject dominate over the fluid motion produced by the free convection mechanisms. It is for this reason that the experimentally determined convective heat and mass transfer coefficients from many calorimeter experiments are averaged and called natural motion limit convective heat and mass transfer coefficients.

#### Report Presentation Format

Section II will deal with the energy balance and transport rate equations. From these equations and the experimental data generated from test subjects, average values of convective heat and mass transfer coefficients are determined. In Section III, additional experimentally determined physiological data will be examined to establish the criteria of human comfort which form the basis for prediction of equal comfort states under different environmental conditions. Section IV will show how to generate equal comfort lines on the psychrometric chart for various conditions of air flow rate, metabolic rate, temperature, and humidity based on constant skin temperature and constant percentage of the body's sweat glands that are active. This section will also examine experimental evidence obtained from the calorimeter and other experiments in the light of these predictions. Section V

will show the extension of the predictive technique to include the transient thermal behavior of a shelteree when exposed to a time dependent radiation flux. The energy storage effect of the subject's body and peripheral tissues and the thermal resistance to heat flow within the body are taken into account. A summary and conclusions relative to the work to date and recommendations for follow-on work constitute Section VI.

## II. ENERGY BALANCE AND TRANSPORT RATE EQUATIONS

### Heat and Mass Transfer Rate Equations

The heat balance equation describing the heat exchange between the human body and its surroundings is based on the law of conservation of energy. This can be stated as: the net rate of energy flow across the skin plus the external mechanical work delivered by the human body equals the metabolic rate minus the increase in heat content of the body. This basic relation applies regardless of the source of heat or the nature of its transfer [9]. This statement can be mathematically expressed as:

$$MR - S = E + R + C + W \quad (1)$$

where MR = (Btu/hr) the net rate of metabolic heat production

S = (Btu/hr) the energy storage rate of the body

E = (Btu/hr) rate of evaporative energy loss

R = (Btu/hr) rate of thermal energy loss by radiation

C = (Btu/hr) rate of thermal energy loss by convection

W = (Btu/hr) mechanical work accomplished

The radiative heat output is negligible in the monoman calorimeter and will be omitted in the initial stages of this development. The energy storage rate of the body is taken as zero initially for equilibrium conditions are assumed at the outset. Therefore, the energy balance equation for sedentary subjects (not delivering external work) can be reduced to:

$$MR = C + E \quad (2)$$

The convective heat transport rate equation can be expressed as:

$$C = h_c A (T_s - T_a) \quad (3)$$

where

$h_c$  = (Btu/hr ft<sup>2</sup>°F) is the body area averaged coefficient of heat transfer.

$A$  = (ft<sup>2</sup>) is the human body surface area calculated from DuBois empirical equation [10].

$T_s$  = (°F) is the body area averaged skin temperature.  
(See Appendix 1 for experimental method of determining this value.)

$T_a$  = (°F) is the logarithmic mean average of air inlet and exhaust temperatures and is determined by the following equation (see Appendix 2):

$$T_a = T_s - \frac{T_o - T_i}{\ln \frac{T_s - T_i}{T_s - T_o}} \quad (4)$$

where

$T_o$  = Dry bulb temperature at exit state of the calorimeter.

$T_i$  = Dry bulb temperature at inlet state.

The logarithmic mean average is used in calculating  $T_a$  because there are large air temperature differences between inlet and exhaust states when test subjects are exposed to inlet dry bulb temperatures considerably above or below their skin temperatures and with very low air flow rates.

The evaporative energy transfer rate equation is

$$E = h_m h_{fg} A \times (w_s - w_a) \quad (5)$$

where

$h_m$  = (lb water vapor/hr ft<sup>2</sup>(lb water vapor/lb dry air))  
average convective mass transfer coefficient based on a wet body area of ( $xA$ ).



$h_{fg}$  = (Btu/lb) latent heat of vaporization of saturated water vapor at  $T_s$

$x$  = The fraction of surface body area  $A$  that is completely wet with sweat (moisture loss from the body area is imagined to occur as though the body were divided into two distinct conditions--one portion entirely wet and the remainder dry). Alternatively,  $x$  can be envisioned as a fraction of the sweat glands that are active.\*

$w_s$  = (lb water vapor/lb dry air) humidity ratio that corresponds to saturated air at  $T_s$ .

$w_a$  = (lb water vapor/lb dry air) logarithmic mean average of air outlet and inlet humidity ratios and is calculated by the following equation (see Appendix 2):

$$w_a = w_s - \frac{w_o - w_i}{\ln \left( \frac{w_s - w_i}{w_s - w_o} \right)} \quad (6)$$

where  $w_o$  and  $w_i$  are the humidity ratios of air at exhaust and inlet conditions, respectively.

Upon substitution of Eqs. (3) and (5) in Eq. (2):

$$MR = h_c A (T_s - T_a) + h_m h_{fg} A x (w_s - w_a) \quad (7)$$

In order to apply Eq. (8) to predict equal comfort states for the human, one must determine values of heat and mass transfer coefficients and devise a method of estimating  $x$  and the corresponding value of  $T_s$  under different environmental conditions.

---

\*Strictly speaking, water loss is from respired air, passive secretion from the skin and active sweat glands. For simplicity, the respired and passive skin losses are considered as an equivalent fraction of active sweat glands.

### Natural Motion Limit

In Reference 1, the natural motion limit concept for convective heat and mass transfer coefficients was established. Attempts to correlate these coefficients from experimental evidence produced by the calorimeter on the basis of natural or forced convection parameters proved unsuccessful. It was concluded that the natural body movements of the subject were inducing boundary air motions which were overriding the weaker fluid forces produced by buoyant or mechanical means (5-15 cfm/person). Hence, for the very low air flow rates, limiting values of the heat and mass transfer coefficients can be assumed as constants. Obviously, when the buoyant or mechanical induced fluid forces create heat and mass transfer coefficients that exceed these limits, the constancy of the values will no longer pertain.

### Evaluation of Convective Heat Transfer Coefficient

The natural motion limit convective heat transfer coefficient  $h_c$  is determined directly from the calorimeter experiments by using the following equation:

$$h_c = \frac{C}{A (T_s - T_a)} \quad (8)$$

The value of C is found by measuring air flow rate and change in sensible air state between inlet and exit. The average value of  $h_c$  for all tests is found to be equal to a .76 Btu/hr  $ft^2 \cdot ^\circ F$ .

### Evaluation of Convective Mass Transfer Coefficient and Per Cent Active Sweat Glands

In the sweating region when the skin is not completely wet, it is very difficult to compute precise values for  $h_m$  and x.

There are no reliable direct methods or instruments known to the authors to measure the value of  $x$ . An attempt was made to evaluate  $h_m$  by asking test subjects to estimate the wetness of their bodies from which a determination of  $x$  could be made. Evaluation of many test results [8] revealed that this method was highly inaccurate as was evident from data scatter and as will be discussed later, resulted in an overestimation of  $x$ .

An improved technique is involved in the present study. First, the  $h_m x$  product is determined and then plotted against average skin temperature,  $T_s$ . The value of  $h_m x$  can be readily determined, independent of test subject response, with reasonable accuracy directly from the calorimeter data. Since  $h_m$  is dictated by test conditions described as natural motion limit conditions,  $h_m$  is assumed constant for all tests. The variation of the product  $h_m x$  with  $T_s$  will then represent only the variation of  $x$  until the whole body is completely wet and  $x$  becomes unity. Beyond this point,  $x$  remains constant, the human body is no longer able to compensate for atmospheric conditions by sweating and the deep body and skin temperature must rise until symptoms of heat stroke appear.

By plotting the values of  $h_m x$  versus  $T_s$  for all tests and fitting curves to this data the  $h_m x - T_s$  relation shown in Fig. 2 is obtained. The asymptotic horizontal line gives the value of  $h_m$  since  $x$  is unity here. The natural motion limit value of  $h_m$  is found from Fig. 2 to be 1.4 lbm water vapor/hr ft<sup>2</sup> (1bm water vapor/lb dry air). With the value of  $h_m$  known, the relation of  $x$  only versus  $T_s$  can be established, as shown in Fig. 3.

## AVE. MASS TRANSFER COEF. VS. SKIN TEMPERATURE

$H_M X$ : BODY AREA AVERAGED MASS TRANSFER COEF.  
LBS. WATER VAPOR/HR FT<sup>2</sup> (LBS WATER VAPOR/LB DRY AIR)  
 $T_S$ : BODY AREA AVERAGED SKIN TEMPERATURE °F

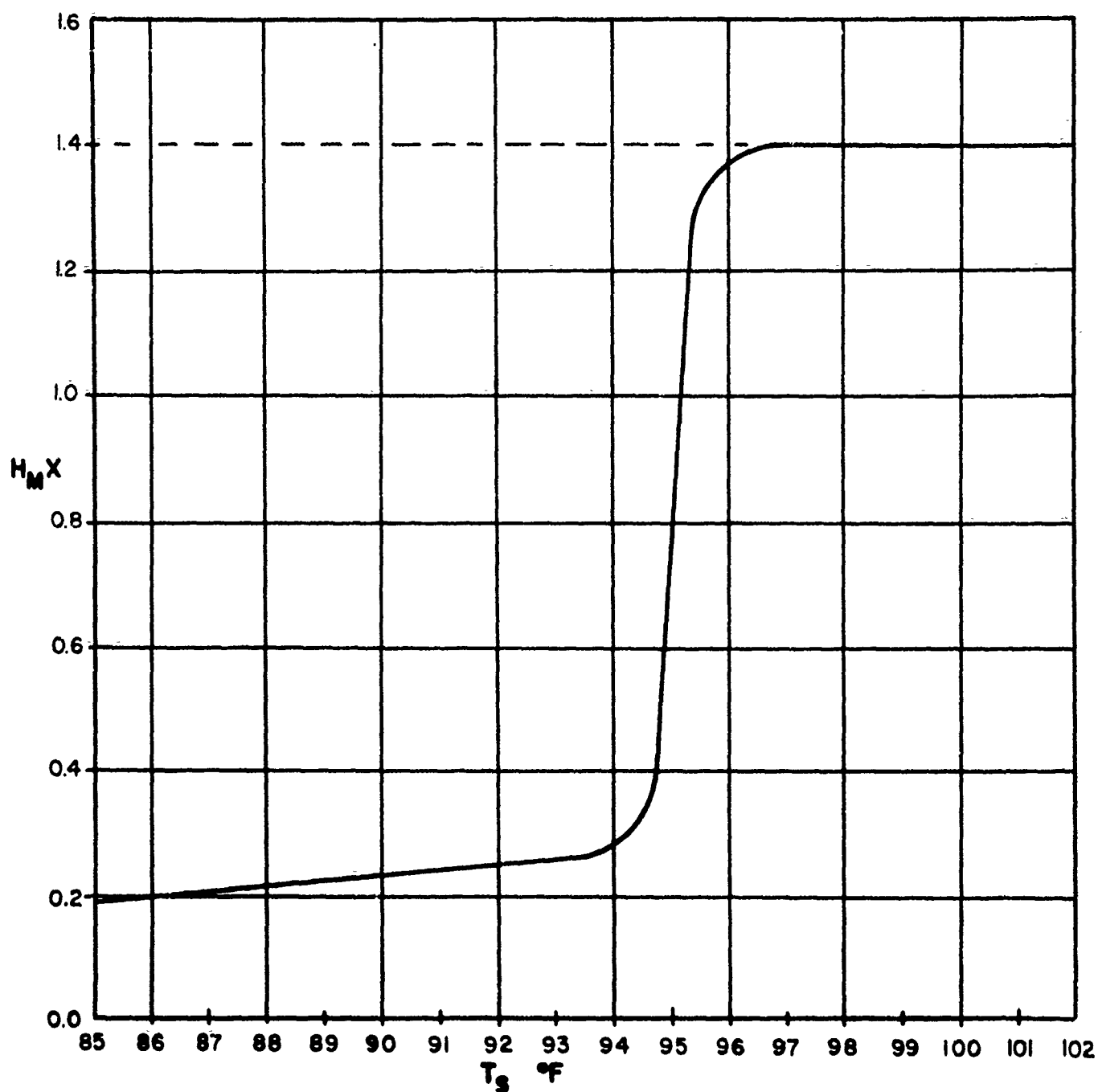


FIGURE 2

# BODY WETNESS FRACTION VS. SKIN TEMPERATURE

14

X: FRACTION OF SKIN SURFACE THAT IS WET

$T_s$ : BODY AREA AVERAGED SKIN TEMPERATURE °F

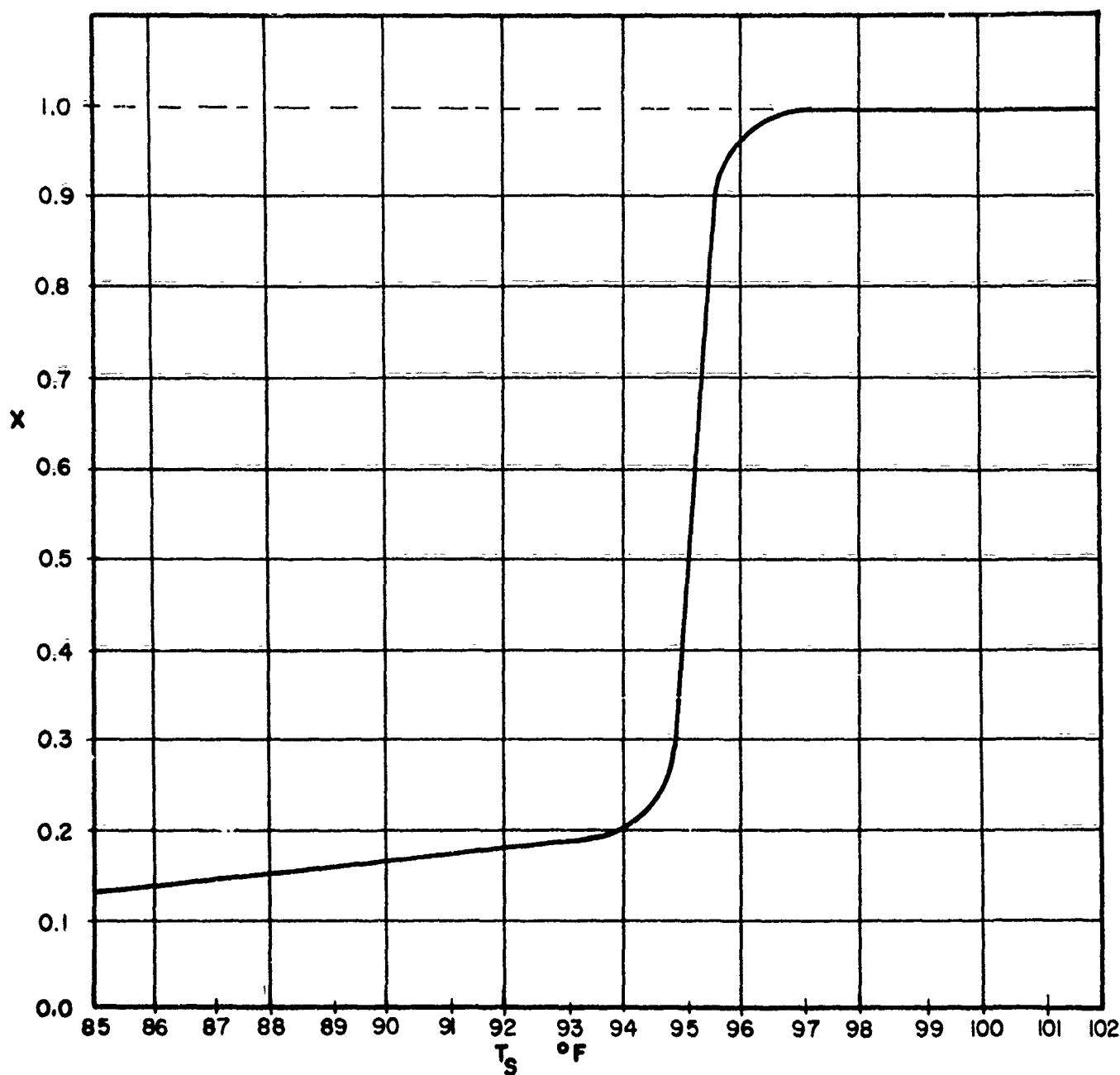


FIGURE 3

### III. THE RELATIONSHIP BETWEEN $(x - T_s)$ AND STATES OF EQUAL COMFORT

Studies have been made of the behavior of evaporation rates from the human body under various environmental conditions. One of these studies was by C. E. Winslow, O. P. Herrington and A. P. Gagge [11]. They found the total evaporative heat loss is independent of atmospheric humidity but dependent on air temperature. This can be explained by physiological control of sweat secretion. If the surface of the body maintains the same physiological characteristics, i.e., maintains the surface wetness and skin temperature, there would be less evaporation with high relative humidity. The rate of evaporation from a unit area of wet surface is proportional to the difference between water vapor concentration at the surface and that of the surrounding air providing air movement is constant. The constancy of evaporative heat loss with varying relative humidity must be maintained by change in sweat secretion. As the humidity ratio of the surrounding environment is increased, there occurs within a given area an increase in the number of active sweat glands, and additional glands are recruited in previously nonsweating areas. This increase in the number of the active sweat glands continues with more severe environments until the limit is reached; the recruitment of sweat spreads to all skin surfaces.

It should be noted from Fig. 3 that there is a slight rise in skin temperature as the sweat glands are recruited. Since this results in a small reduction in convective heat transfer, the evaporative heat loss will increase slightly as the air humidity increases. From a strict point of view, the finding of Winslow, et al., is not correct.

### Interpretation of $(x - T_s)$ Relationship

In Section II the relation between skin wetness,  $x$ , as the fraction of the body surface that is covered by an evaporative thin film of sweat, and the average skin temperature was established; see Fig. 3. This is the principal physical property relationship of the boundary skin surface and is the resultant of both various internal regulatory processes and the external stress caused by the environment. Therefore, every point on the  $(x - T_s)$  curve of Fig. 3 is a unique physiological comfort or discomfort condition. If the human body is exposed to different environmental conditions that would keep the value of  $T_s$  and the corresponding value of  $x$  constant irrespective of the heat exchange mechanism, then these different environmental states can be defined as states of equal comfort.

### Subdivision of the $(x - T_s)$ Relationship

The  $(x - T_s)$  relation can be divided into three distinct regions:

(1) Insensible or Passive Sweating Region. This region is bounded by a skin temperature below 94°F and above the shivering point. The skin wetness is almost constant due to the absence of sweat secretion. The skin temperature is the dominant thermal regulatory control, i.e., the body temperature regulation is mainly by change in skin temperature. There is some uncertainty as to whether or not there is an exact value of the critical skin temperature at which sweat secretion starts. This is due to the lack of sufficient tests around this critical point. Hence, the transition between insensible and sensible sweat regions is not

known precisely as to whether it is a smooth or abrupt transition. There is some evidence based on tests of one individual to support the view that the transition is smooth, i.e., in the transition region active sweating is conditioned by gradual rise in skin temperature after which the rate of increase of sweat secretion with skin temperature reaches a maximum value.

(2) Modulated Active or Sensible Sweating Region. This region is bounded by  $T_s$  between  $94^{\circ}\text{F}$  and  $96.2^{\circ}\text{F}$ . As mentioned above, in this region the rate of increase of wetness with skin temperature reaches maximum limit. In other words, the rise of skin temperature is very small compared to the increase of  $x$ . This occurs because the sweat glands suddenly begin to secrete and are able to dissipate heat by evaporation so successfully that no further significant rise in skin temperature occurs.

(3) Heat Stroke Region. In this region,  $T_s > 96.2^{\circ}\text{F}$ , there is a loss of thermal regulation. The body surface is completely wet and the body is no longer able to dissipate more heat by evaporation even though the sweat secretion increases. Under this condition the skin temperature starts to rise in a fashion similar to region 1. Since no further body surface regulation is possible, the deep body temperature will also rise until the body exceeds high temperature tolerance and heat stroke begins.

In the present analysis, only regions one and two are considered, since it is in these two regions only that the body maintains normal thermal regulatory equilibrium with the environment.

In summary, the principal phenomena observed from the physiological relation of  $(x - T_s)$  are:



- (a) The triggering of the active sweat secreting mechanisms is intimately related to a critical skin temperature. The average value of this critical temperature is in the vicinity of  $94^{\circ}\text{F}$ .
- (b) There are two major thermal regulatory controls on the human body surface, namely, the skin temperature and sweat secretion.
- (c) Points on the  $x - T_s$  graph define different settings of the body's thermoregulatory function and hence are points of thermal comfort or discomfort.

#### Physiological Thermal Index

Values can be assigned to points on the  $(x - T_s)$  relation to give the level of physiological strain or level of external environmental stress. Any value from the physiological scale, a point on the  $(x - T_s)$  curve, represents a fixed physiological state regardless of the particular environment which produces this state. Because there are two different thermal regulatory controls on the human body surface, one the sensible heat regulatory control,  $T_s$ , and the other the evaporative heat control,  $x$ , a reasonable index should weigh these two thermal regulatory controls equally according to their power to dissipate the metabolic heat output under the same environmental condition. The method proposed to evaluate the heat dissipating power by varying  $T_s$  as compared to varying  $x$  is to calculate the ratio of metabolic heat output dissipation by unit change in  $T_s$  and assign a unit to a change in  $x$  that will result in an equal heat dissipating power. From this heat dissipating power ratio, increments

of  $x$  and  $T_s$  can be weighed accordingly on the scale. The heat dissipating power ratio is derived as follows:

Under constant environmental conditions, the metabolic rate is a function of  $T_s$  and  $x$ . This function can be written as:

$$MR = f(T_s, x) \quad (9)$$

This relation shows that if metabolic heat output of a human body is incrementally shifted while holding a constant environment, the only way to dissipate this increased amount of heat output is by change in the values of  $T_s$  and  $x$ . This incremental change in metabolic rate can be expressed as follows:

$$dMR = \left(\frac{\partial f}{\partial T_s}\right)_x dT_s + \left(\frac{\partial f}{\partial x}\right)_{T_s} dx \quad (10)$$

if  $dMR = 0$ .

$$\text{Therefore, } \frac{dx}{dT_s} = - \frac{\left(\frac{\partial f}{\partial T_s}\right)_x}{\left(\frac{\partial f}{\partial x}\right)_{T_s}} \quad (11)$$

From Eqn. (7) ,

$$\left(\frac{\partial f}{\partial T_s}\right)_x = h_c A \quad (12)$$

and

$$\left(\frac{\partial f}{\partial x}\right)_{T_s} = h_m h_{fg} A (w_s - w_a) \quad (13)$$

Upon substituting Eqs. (12) and (13) into Eqs. (11),

$$\frac{dx}{dT_s} = - \frac{h_c}{h_m h_{fg} (w_s - w_a)} \quad (14)$$

Equation (14) shows  $\frac{dx}{dT_s}$  is dependent on air humidity, i.e., the cooling power ratio of evaporation to convective heat transfer varies with the air humidity. The evaporation rate per unit surface area is a maximum when air humidity is zero and it is

minimum when the air humidity ratio is equal to that at the skin surface. The proposed index is built by choosing a value for  $\frac{dx}{dT_s}$  which is evaluated at  $w_a$  equal to zero. As a first approximation, the right-hand side can then be assumed a constant with  $h_{fg}$  and  $w_s$  evaluated for  $T_s = 95^\circ\text{F}$  and substituting the experimentally determined values of  $h_c$  and  $h_m$  in Eqn. (14), the result is:

$$\frac{dx}{dT_s} = - \frac{1}{70} (^\circ\text{F})^{-1} \quad (15)$$

Equation (15) shows that when the surrounding environment is completely dry, a change of  $x$  from zero to completely wet body surface is equivalent to a rise of  $70^\circ\text{F}$  in skin temperature.

With the heat dissipating power ratio established, the physiological index can be constructed. The zero point on the index is taken to be the point on  $(x - T_s)$  curve of skin temperature of  $93.4^\circ\text{F}$ . The corresponding body temperature under equilibrium condition is found to be  $97.9^\circ\text{F}$  [15]. The values  $93.4^\circ\text{F}$  and  $97.9^\circ\text{F}$  have been observed as the average temperatures of the skin and deep body, where there is minimal regulatory effort in maintaining body temperature either by any vascular effort or by sweating. When these temperatures occur simultaneously during rest, the body is in a state of "Physiological Thermal Neutrality" [14]. Above this natural point, the body will sense warmth and the reading on the index will be positive and below it the body will sense coolness and the reading on the index will be negative. The index is divided in such a way that one division represents a change of .05 in  $x$  or  $3.5^\circ\text{F}$  change in  $T_s$  or combinatorial change of  $T_s$  and  $x$  weighted according to their heat dissipating power. The index is superimposed

on ( $x - T_s$ ) relation as shown in Fig. 4. Each division on the index represents equal amounts of metabolic heat output that can be dissipated by physiological change of  $x$ ,  $T_s$ , or both. This scale is defined as the Physiological Thermal Index (PTI).

In Section IV the PTI is combined with the environmental conditions through heat and mass transfer rate equations to predict environmental states of equal comfort. These states of equal comfort are defined as the air state that would result in the same values of  $x$  and  $T_s$ .

Numerous problems have been identified and numerous attempts have been made to improve the effective temperature concept, some of which have been cited previously. One of the most serious difficulties associated with the effective temperature and other indices of comfort is that they are tied to environmental conditions as part of their basic definition. With the Physiological Thermal Index established independently of environmental conditions, it becomes the primary index of human comfort. The same PTI line will be located at different positions on the psychrometric chart depending upon metabolism, air flow rate, temperature, humidity and radiation factors. Yet, the line will represent the same index value on the  $x - T_s$  relationship and hence a constant index of comfort.

PHYSIOLOGICAL THERMAL INDEX (PTI) SUPERIMPOSED ON X VS.  $T_s$ 

X : FRACTION OF BODY SKIN SURFACE THAT IS WET

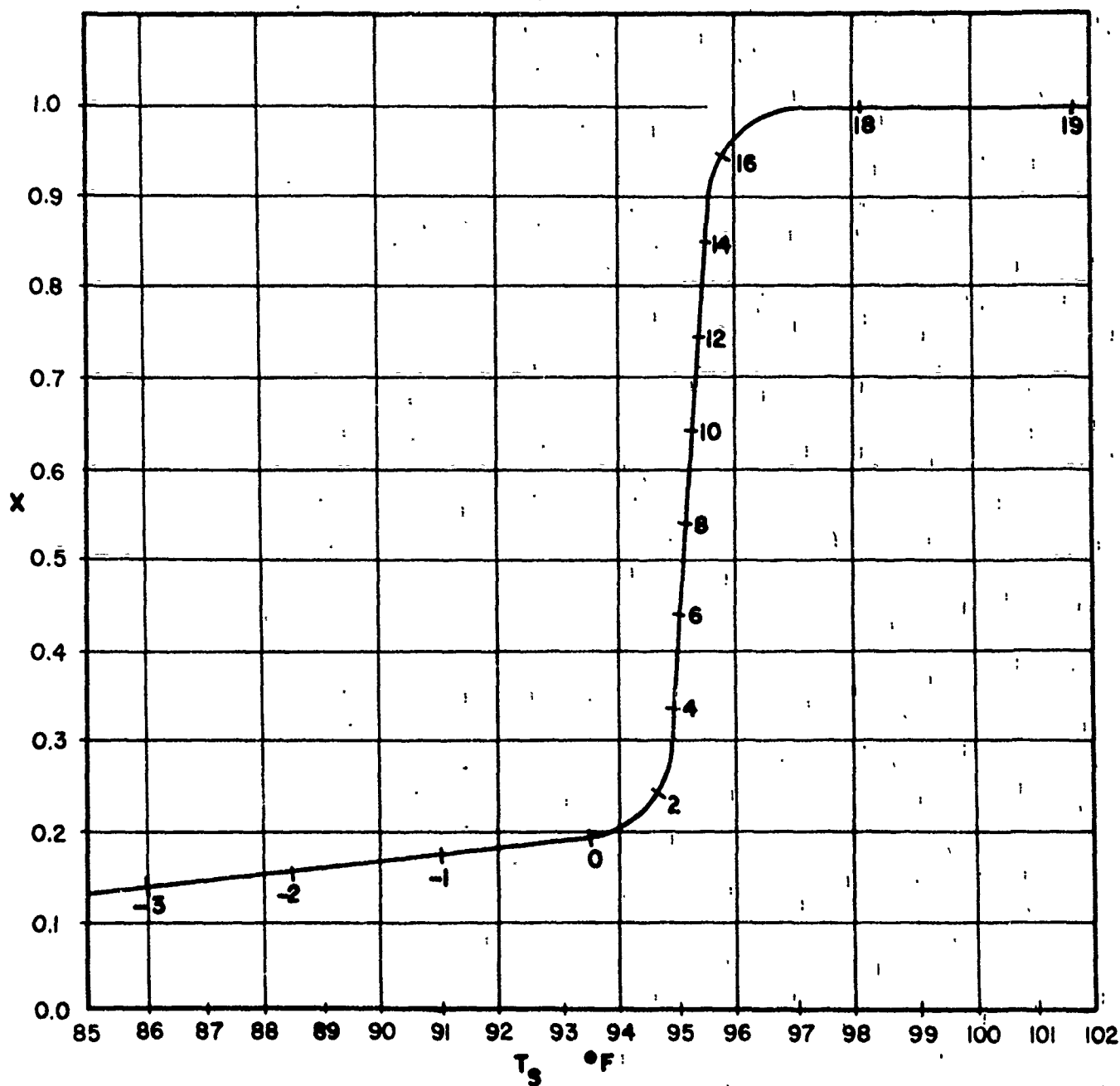
 $T_s$  : BODY AREA AVERAGED SKIN TEMPERATURE °F

FIGURE 4

#### IV. THE LOCI OF PTI VALUES ON THE PSYCHROMETRIC CHART

In locating lines of constant PTI values on the psychrometric chart the following simplifications and assumptions are made:

- (1) The specific heat and molecular weight of dry air are used in place of the water vapor-dry air mixture values, since the mixture contains no more than 3 per cent water vapor by weight.
- (2) The total evaporative heat losses which include heat of vaporized moisture from the lungs during respiration, heat of vaporized water diffusing through skin layer and the heat of vaporized sweat necessary for the regulation of body temperature are taken as one quantity and represented by a fraction,  $x$ , of the skin that is assumed saturated.
- (3) The human body is in steady state with the environment, i.e., the average skin temperature, deep body temperature and metabolic rate are not varying with time.
- (4) The humidity ratio at the wet skin surface is determined assuming a saturated condition at skin temperature,  $T_s$ .

##### Derivation of Psychrometric Equations Using PTI Values

The generated lines of equal comfort are based on average environmental conditions. In the human calorimeter, which is a relatively confined space, or in shelters with minimum ventilation, the test subjects (due to their energy and moisture release) will experience significant differences between the initial air state as it contacts their body and final air state as it leaves their body. For this reason the logarithmic average of inlet and exhaust states is assumed as the average air condi-

tion to which the test subject is exposed. Sensible and evaporative heat outputs and average air states are calculated in terms of the inlet and exit air states by the following equations:

Sensible heat is calculated in terms of air mass flow rate, inlet and exhaust dry bulb temperature by

$$C = G C_p (T_o - T_i) \quad (16)$$

where  $G$  (lbm/hr) is the air mass flow rate.  $C_p$  (Btu/lbm°F) is the specific heat of dry air at constant pressure.

From Eqs. (3) and (4),  $C$  can be rewritten as:

$$C = h_c A \frac{T_o - T_i}{\ln \left( \frac{T_s - T_i}{T_s - T_o} \right)} \quad (17)$$

Combining Eqs. (16) and (17),  $T_o$  can be written in terms of  $T_i$  as follows:

$$T_o = T_s (1 - e^{-Y}) + T_i e^{-Y} \quad (18)$$

where

$$Y = \frac{h_c A}{G C_p}$$

Substituting Eq. (18) into Eq. (17),  $C$  can be recast in terms of inlet dry bulb temperature, mass flow rate and convective heat transfer coefficient, as:

$$C = G C_p (T_s - T_i) (1 - e^{-Y}) \quad (19)$$

The total evaporative heat loss can also be related to humidity ratios at inlet and exit states and air mass flow rate by the following equation:

$$E = G h_{fg} (w_o - w_i) \quad (20)$$

Upon substitution of Eq. (6) into Eq. (5), E can be rewritten as:

$$E = h_m h_{fg} A x \frac{w_o - w_i}{\ln \left( \frac{w_s - w_i}{w_s - w_o} \right)} \quad (21)$$

Combining Eqs. (20) and (21),  $w_o$  can be written in terms of  $w_i$  as follows:

$$w_o = w_s - (w_s - w_i) e^{-Z} \quad (22)$$

where

$$Z = \frac{h_m A x}{G}$$

Substituting Eq. (22) into Eq. (20)

$$E = G h_{fg} (w_s - w_i)(1 - e^{-Z}) \quad (23)$$

From Eqs. (23), (22) and (6), total evaporative heat loss, humidity ratio at exit condition and average humidity ratio can be determined for constant skin temperature and constant wetness, but at varying air mass flow rate, by substituting different values of  $w_i$  in the corresponding equations.

Sensible heat output, C, can be determined by subtracting the evaporative heat loss from the metabolic heat output. Knowing the sensible heat output, mass flow rate, and skin temperature, the inlet dry bulb temperature can be calculated by

$$T_i = T_s - \frac{C}{G C_p (1 - e^{-Z})} \quad (24)$$

Note: The preceding relations are applied to calculate the inlet and exit air states under various air flow rates. The average air state, sensible and evaporative heat output can be held constant while varying inlet states and the air flow rates.



A computer program is written (see Appendix 3) to compute average air states, sensible and evaporative heat outputs, inlet and exit air states that correspond to constant skin temperature and constant wetness, i.e., air states of equal comfort. Metabolic rate may also be varied as a program parameter.

#### Generation of Lines for PTI Constant Values

Two sets of PTI constant lines are generated by the computer program. One set, shown in Fig. 5, represents a typical population sample (based on 1960 United States Census [12]) which has an average metabolic rate of 275 Btu/hr [1] and surface area of 15.6 ft<sup>2</sup>. The other set, shown in Fig. 6, represents adult males with average metabolic rate of 400 Btu/hr [13] and surface area of 20 ft<sup>2</sup>. C. P. Yaglou's ET lines for nude and clothed subjects [17] are drawn in both Figs. 5 and 6, as comparisons to the predicted PTI constant lines.

#### Characteristics of Predicted PTI Lines

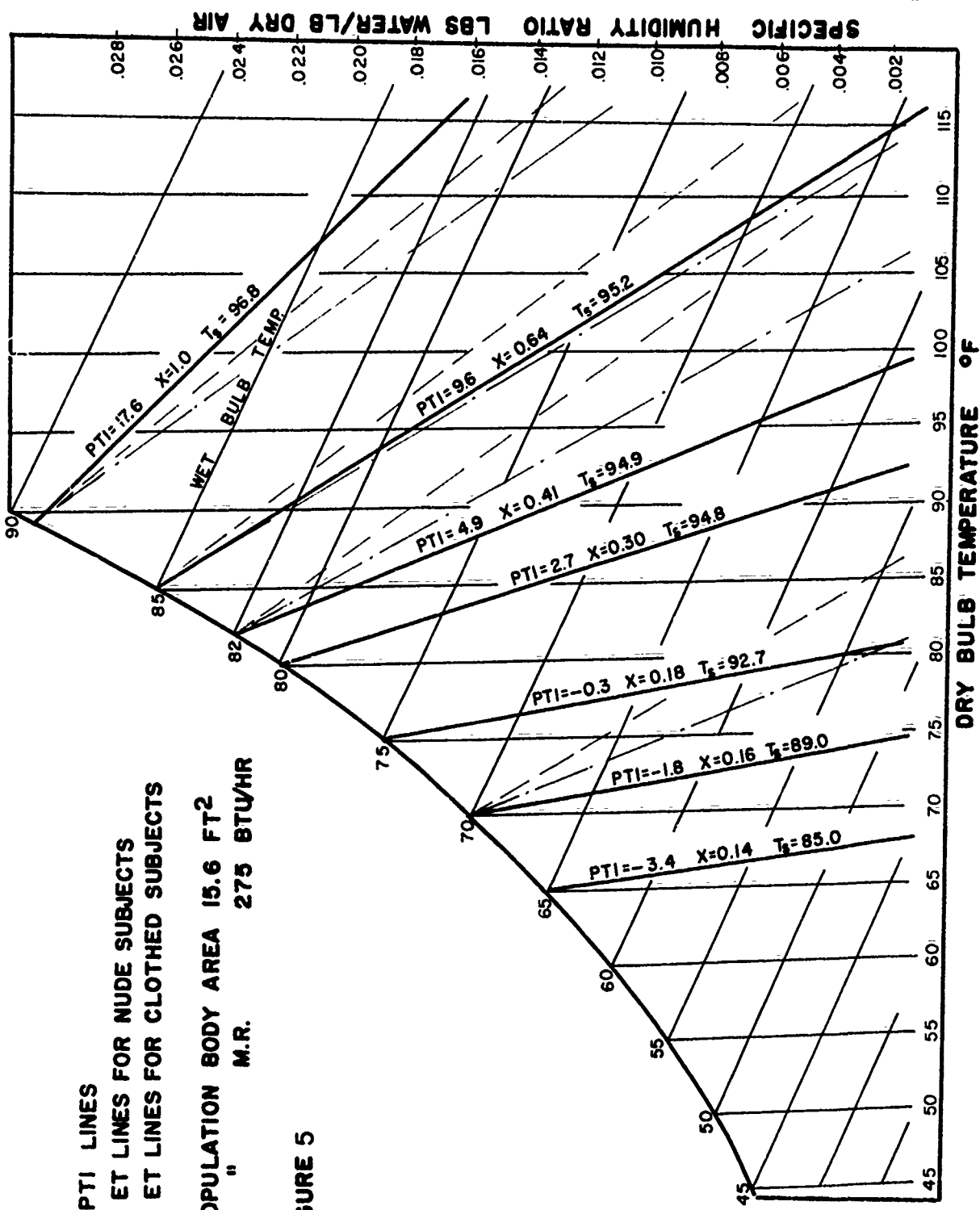
The predicted PTI lines (loci of constant skin temperature and constant wetness) are shown as solid lines in Fig. 5. The constructed PTI lines cover the range of slightly cool environment (-3.4 PTI line) to the maximum tolerable limit where the body is completely wet. This maximum limit is represented by the 17.64 PTI line. It is noticed, in the slightly cool environment that the PTI lines are very steep. As the PTI value increases the slope of the line decreases to a minimum value which is represented by the 17.64 PTI line. Beyond this PTI line the slope remains the same because the surface wetness remains constant ( $x = 1$ ) and the skin temperature rises.

# PREDICTED NUDE PTI LINES FOR GENERAL POPULATION USING X-T<sub>s</sub> CURVE

- PREDICTED PTI LINES
- - - C.P. YAGLOU ET LINES FOR NUDE SUBJECTS
- · - C.P. YAGLOU ET LINES FOR CLOTHED SUBJECTS

GENERAL POPULATION BODY AREA 15.6 FT<sup>2</sup>  
 " " M.R. 275 BTU/HR

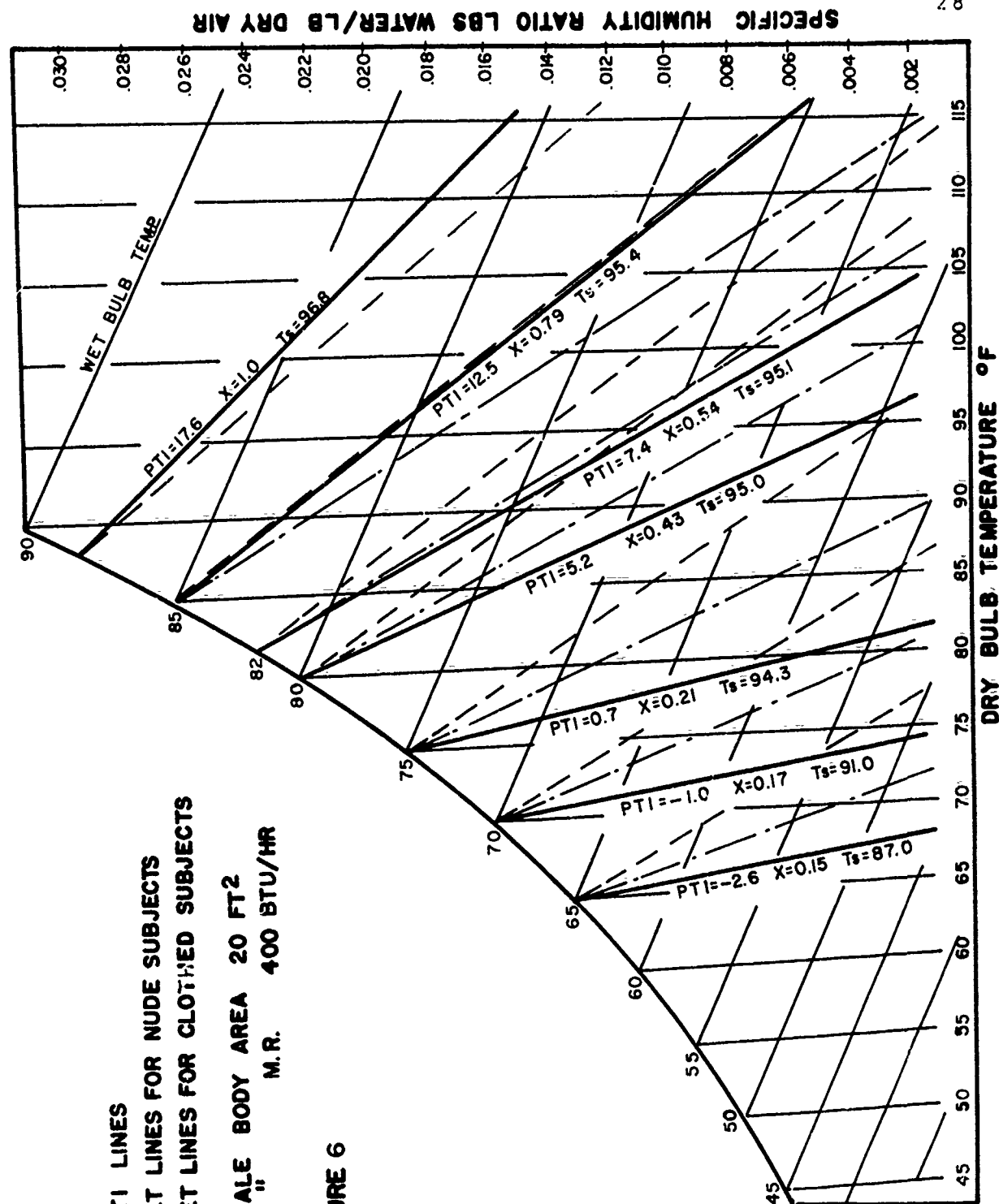
FIGURE 5



# PREDICTED NUDE PTI LINES FOR ADULT MALES USING $X-T_s$ CURVE

- PREDICTED PTI LINES
  - - - C.P. YAGLOU ET LINES FOR NUDE SUBJECTS
  - - - C.P. YAGLOU ET LINES FOR CLOTHED SUBJECTS
- ADULT MALE BODY AREA 20 FT<sup>2</sup>  
M.R. 400 BTU/HR

FIGURE 6



From this observation, it is concluded that the humidity ratio of the environment has slight effect on comfort at lower PTI values while in the higher PTI range it has a pronounced effect. This can be interpreted by noting that the skin temperature is the dominant index of comfort in the region of insensible sweating while the skin wetness is the dominant index of comfort or discomfort in the active sweating region.

C. P. Yaglou's ET lines are drawn in Fig. 5 in broken lines as a comparison to the predicted PTI lines. But we cannot draw a comparative conclusion between these lines since Yaglou's ET lines are for adult males with different metabolic rates per unit of body area than the general population. Although the generated PTI lines for adult males have the same general trends as that of the general population except as will be discussed later it is more appropriate to limit the comparison only between ET lines for nude adult males generated by Yaglou and by our predictive model.

#### Comparison Between Yaglou's Values and Predicted PTI Lines for Adult Males

A comparison between Yaglou ET lines and PTI lines predicted by the present study can be made by superimposing each set of ET lines on the same psychrometric chart, as shown in Fig. 6. The predicted PTI lines are shown by solid lines while Yaglou lines are shown by broken lines. In the region of lower PTI lines, it is noticed that there is a great deviation between Yaglou lines and the predicted ones. Yaglou lines show a much greater humidity dependence than the predicted lines. In the region of higher PTI lines, Yaglou lines correspond quite well

with the predicted lines, particularly at the 85 ET line. On the other hand, the predicted line of  $x$  equals unity shows greater dependence on humidity than the corresponding Yaglou ET line. From the preceding analysis, we can draw the same conclusion as other workers that Yaglou ET lines overestimate the influence of humidity on sensations of warmth and comfort at ordinary temperatures and underestimate the effect at very high temperatures.

This conclusion can also be arrived at by examining the variation of wetness ( $x$ ) with average dry bulb temperature using the Yaglou ET line as a parameter--see Fig. 7. The wetness  $x$  at any dry bulb temperature along the Yaglou ET line is calculated by the following equation:

$$x = \frac{MR - h_c A (T_s - T_a)}{h_m h_{fg} A (w_s - w_a)} \quad (25)$$

where

MR is the average metabolic rate output of adult males (400 Btu/hr).

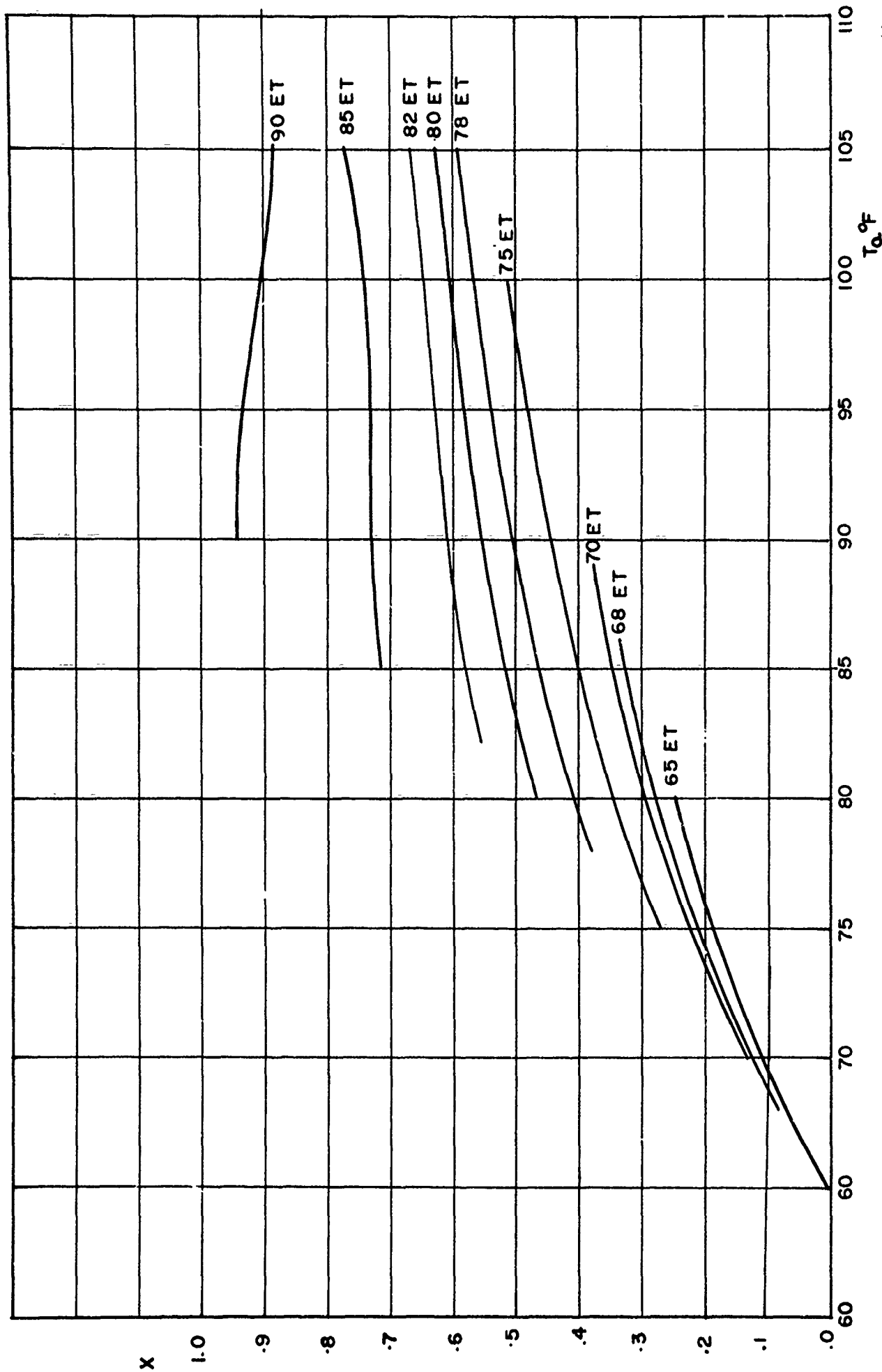
$h_c$  is the experimentally determined convective heat transfer coefficient (.76 Btu/hr).

A body surface area for average adult male (20.0 sq ft).

$h_m$  Experimentally determined convective mass transfer coefficient (1.4 lb water vapor/hr ft<sup>2</sup> (lb water vapor/lb dry air)).

$h_{fg}$  latent heat of vaporization at the partial pressure of saturated water vapor at  $T_s$ .

$T_a$  air dry bulb temperature at a point on Yaglou ET line that corresponds to  $T_a$ .

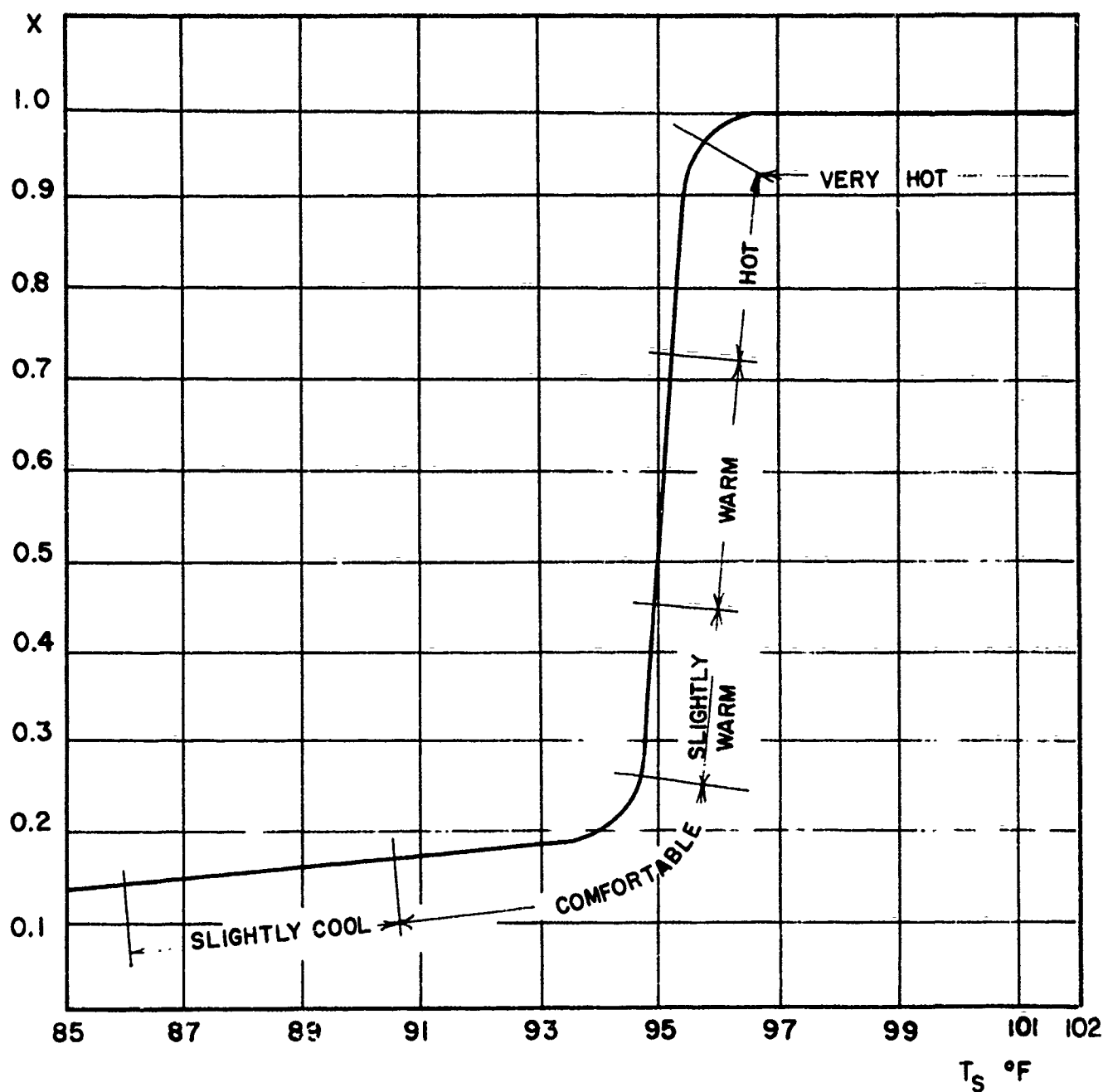


VARIATION OF  $X$  WITH C.P. YAGLOU ET LINES FOR NUDE GENERAL POPULATION AND VERY LOW FLOW RATE

FIGURE 7

$X$ : FRACTION OF BODY SKIN THAT IS WET

$T_s$ : BODY AREA AVERAGED SKIN TEMPERATURE °F



THERMAL COMFORT ZONES ON ( $X$ - $T$ ) CURVE

FIGURE 8

COMFORT ZONES FOR SEMI-NUDE ADULT MALES  
UNDER VERY LOW AIR FLOW RATES

FIGURE 9

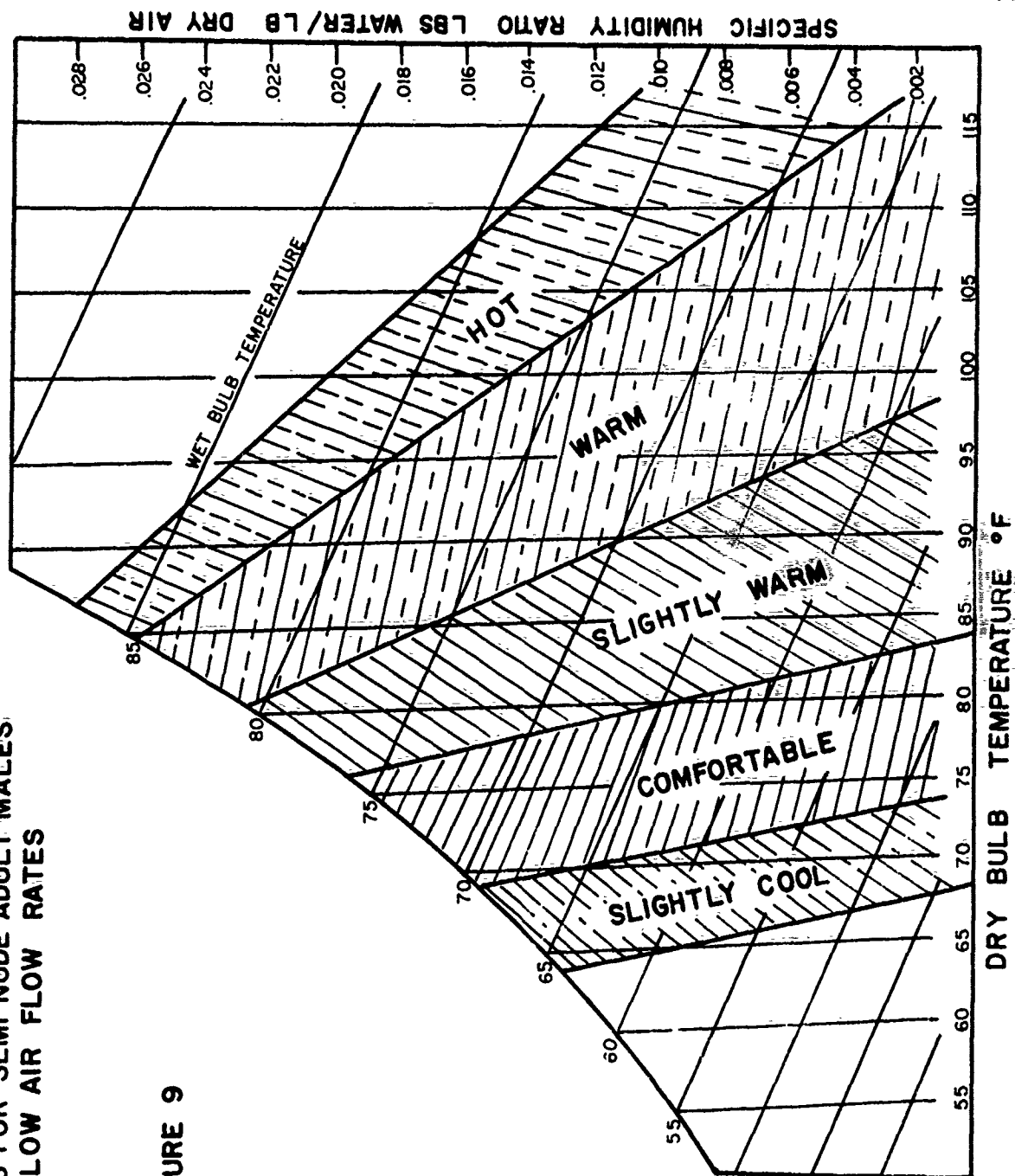




Fig. 10. Our predictive PTI lines and F. Rohles and R. Nevins comfort lines [22] are also drawn in Fig. 10 for comparison. It should be pointed out that Nevins and Gagge used different valued environmental parameters than we used. The present study deals primarily with semi-nude people under the environment of very low ventilation rates and in the absence of radiation exchange, while Gagge and Nevins used the environmental characteristics of lightly clothed people and wall temperatures equal to air temperature. Therefore, the predicted PTI lines and Gagge's new ET lines that coincide do not necessarily represent the same level of comfort. But the important observation noticed from Fig. 10 is that the PTI lines have the same slopes as those of Gagge, i.e., they agree well on humidity dependence and on thermal sensation.

#### Subjective Experimental Response Compared to the New PTI Lines

At the time the new PTI lines were being developed some tests in the lower temperature range were performed on subjects in the monoman calorimeter with each test consisting of two parts. In the first part, the inlet dry and wet bulb temperatures were chosen and kept constant during that part of the test and data was collected after the subject reached equilibrium with his environment. The second part of the test consisted of keeping the dry bulb temperature the same as that of the first part of the test and changing the wet bulb temperature to a different value. After the subject reached equilibrium in the second part of the test, verbal expressions were obtained from the subjects regarding their sense of hotness, coolness or comfort to the first state. Surprisingly, most of the answers from the test subjects were that they sensed the same comfort as that

# PREDICTED NUDE PTI LINES FOR ADULT MALES COMPARED WITH GAGGE AND KSU

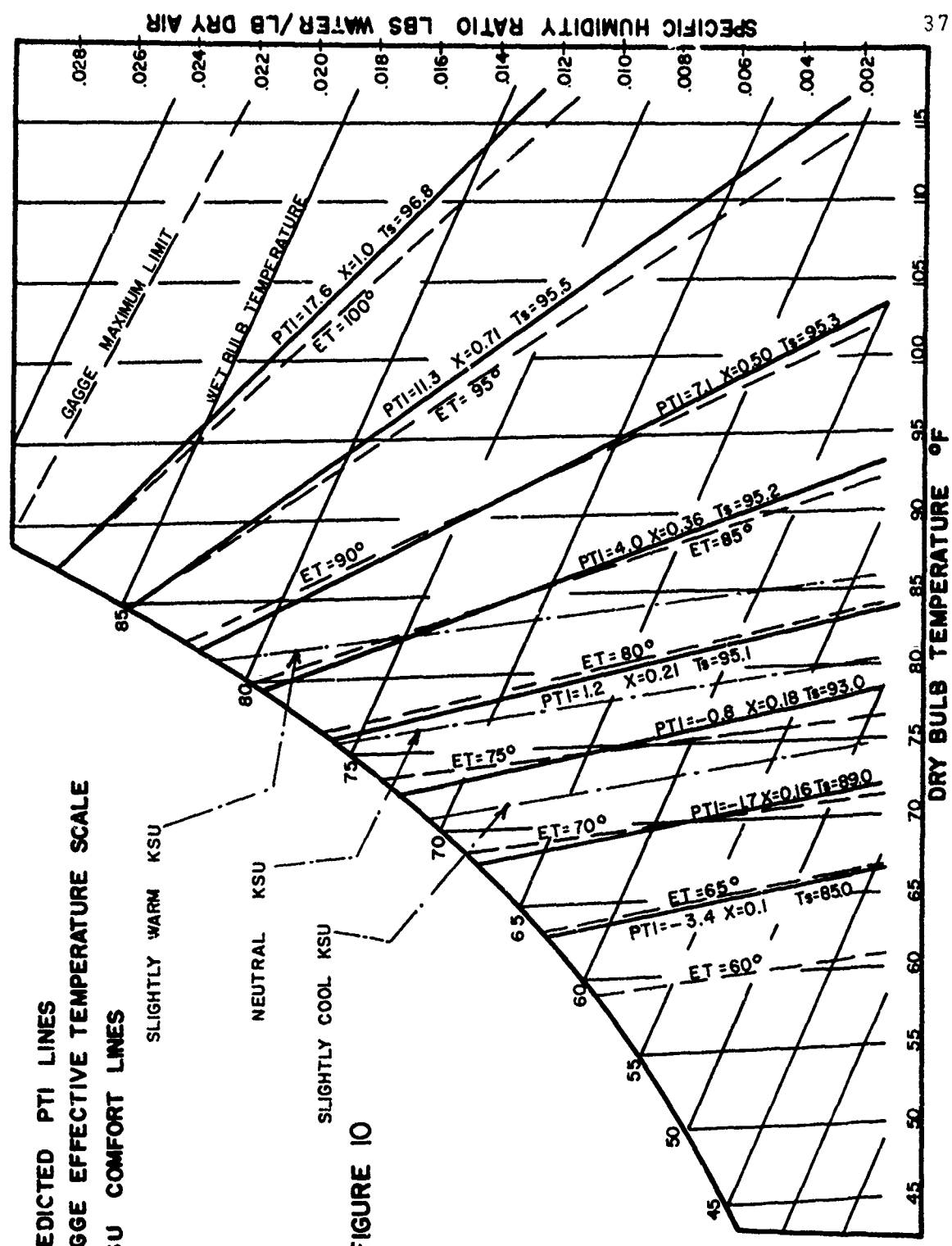
- PREDICTED PTI LINES
- - - GAGGE EFFECTIVE TEMPERATURE SCALE
- · - · - KSU COMFORT LINES

SLIGHTLY WARM KSU

NEUTRAL KSU

SLIGHTLY COOL KSU

FIGURE 10



of the first part of the test even though the majority did observe the change in humidity. From these tests it appears that the humidity has little effect on comfort in the normal temperature range. This supports the new method for prediction of the PTI lines. Although the number of these tests is limited to date, they give significant support to the concepts underlying the physiological thermal index.

Work conducted during this project but previous to the creation of the predictive model involving the PTI index lends further support to the worth of the concept.

Comparisons of psychological impressions with physical environment were attempted in 32 pairs of tests in which the test subject was exposed sequentially to two different climate states. The test conditions were 82 and 85°F ET air inlet state and 13 cfm. Subject thermal equilibrium was established for each test state. These sequential states were usually on the same effective temperature line. There were 21 pairs of tests with constant effective temperatures and 11 pairs of tests with differing effective temperatures. The high and low humidity sequences were alternated from one pair of tests to the next.

After experiencing the two climate states, the subject was asked to check one item in the following statement:

"How does the new condition compare with the first condition of about an hour ago? More comfortable \_\_\_\_ Less comfortable \_\_\_\_ Same \_\_\_\_."

In effect, the subject would have three equally possible responses if the response were random compared to a measured physical parameter. That is, the most probable number of

responses of one classification to the total number of responses would be one-third if there were no correlation.

A. Response Compared to Test Sequence

Those who indicated 1st state was less comfortable	7/32	22%
Those who indicated 2nd state was less comfortable	8/32	25%
Those who indicated the states were the same	17/32	53%

B. Response Compared to ET

Those whose impression agreed with the change in effective temperature	21/32	66%
--	-------	-----

C. Response Compared to  $q_l$  (latent heat)/ $q_t$  (total heat)

Those who felt warmer for higher $q_l/q_t$	5/32	16%
Those who felt cooler for higher $q_l/q_t$	10/32	31%
Those who felt the same for higher $q_l/q_t$	17/32	53%

D. Response Compared to Skin Temperature\*

Those who were less comfortable with higher skin temperature	7/28	25%
Those who were more comfortable with higher skin temperature	6/28	21%
Those who felt the same with higher skin temperature	15/28	25%

Plausible Conclusions

1. Test sequence is not a significant factor in the test subject's response.
2. Effective temperature is strongly related to psychological impressions for these test conditions.

---

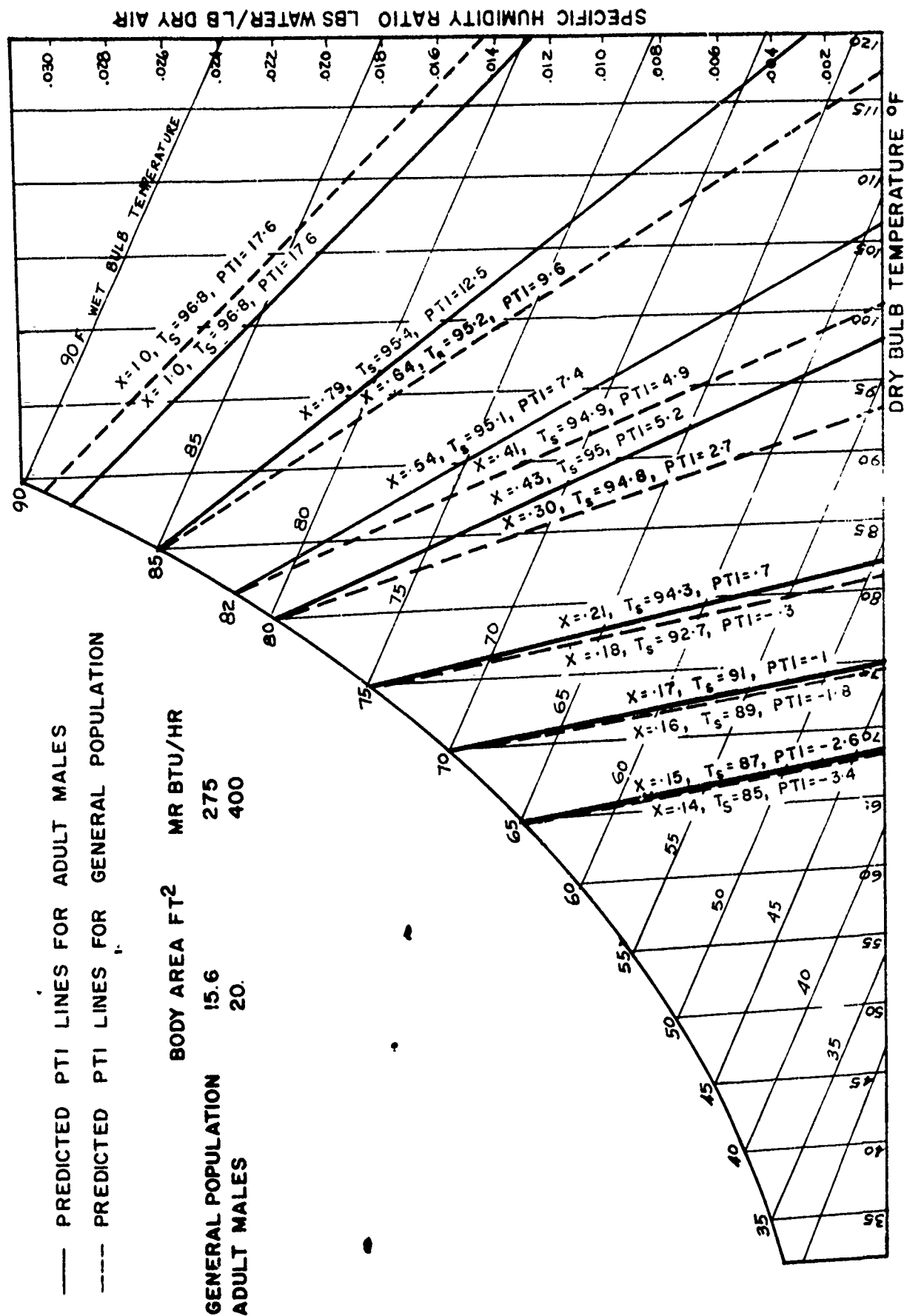
\*The reason for 28 tests here is that some subjects produced the same skin temperature  $\pm 0.1^\circ\text{F}$  which is within the uncertainty estimate of the average skin temperature.

3. The psychological response shows no significant correlation with changes in humidity even though the value of  $q_l/q_t$  was changed in all but one test and as much as 30% in some cases. Likewise, no significant correlation is observed between change in averaged skin temperatures and psychological response. It is to be noted that skin temperature changes for the two test states were usually less than  $1/2^\circ\text{F}$ .

It was shown in Fig. 7 for the  $82-85^\circ\text{F}$  effective temperature range that there was good agreement between the PTI lines and the ET lines. The experimental evidence just cited gives physical testimony as to the correctness of the predictive model in this region and further strengthens the merits of the Physiological Thermal Index concept.

#### Predicted PTI Lines of Adult Males Compared with General Population

The PTI lines for a general population sample and those for adult males are superimposed in Fig. 11. It is interesting to note in this figure that the slopes of PTI lines that lie on the psychrometric chart in the range of  $65-70^\circ\text{F}$  saturation temperature for both adult males and the general population are nearly the same but with significantly different values of  $x$  and  $T_g$ . This means that the effect of humidity on comfort for both adult males and the general population is the same in this range of PTI lines. The different values of  $T_g$  for adult males and general population at  $65^\circ\text{F}$  saturation indicates that they should not sense the same comfort under the same environment due to the difference in their metabolic rate per unit of body surface area. At higher PTI lines adult males show a greater dependence on humid-



PREDICTED PTI LINES OF NUDE ADULT MALES COMPARED WITH GENERAL POPULATION

FIGURE II

ity for their comfort than the general population. Assuming equal acclimatization and tolerance the general population should be able to tolerate more severe environmental conditions than adult males, as is evidenced by contrasting the PTI lines at  $x$  equals unity for adult males and the general population.

The preceding discussion indicates that subjects with different metabolic rates and different body areas may not have the same physiological comfort, as their PTI values will be different under the same environmental conditions.

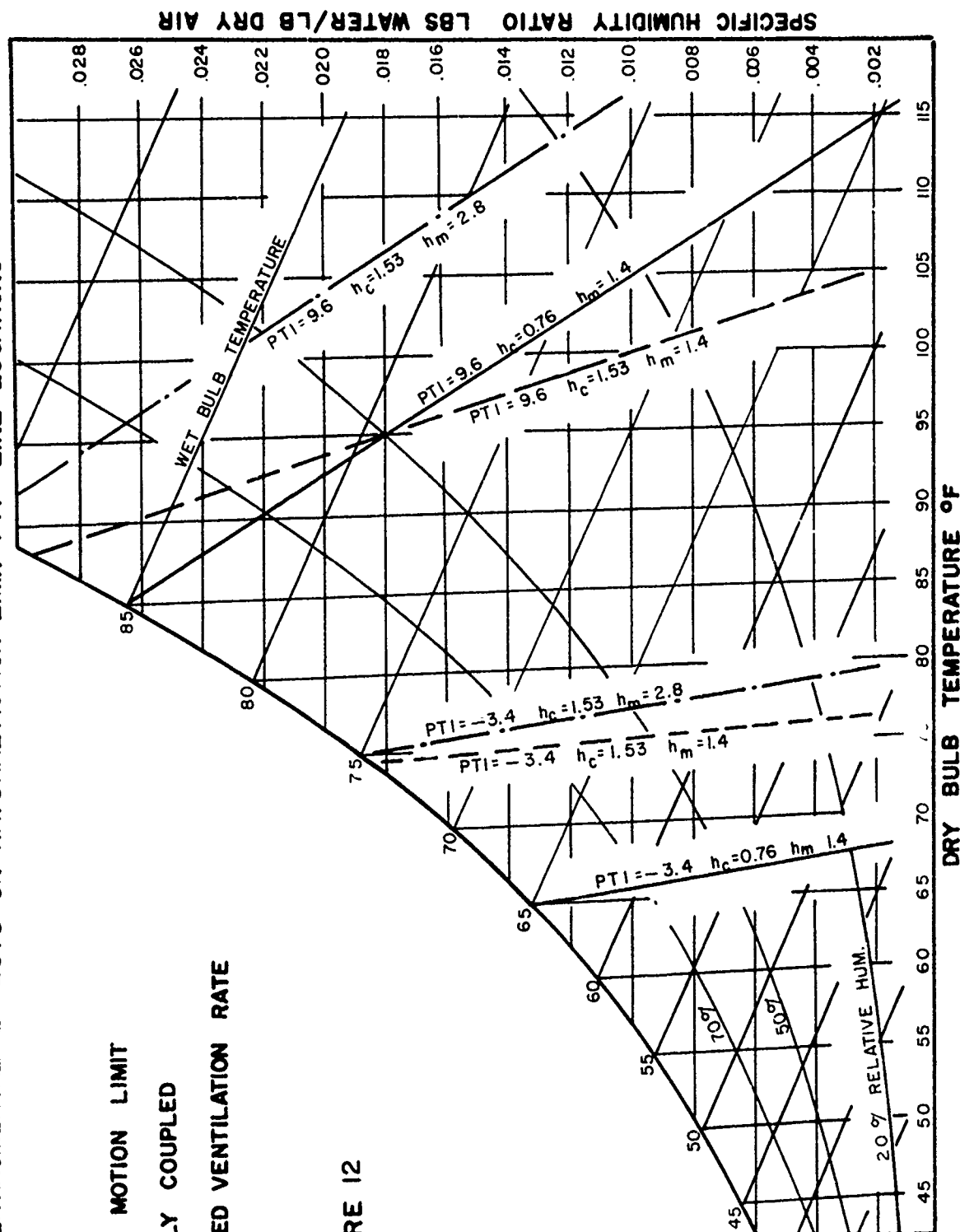
#### Predicted PTI Lines for Subjects in Environments of High Air Velocities and Radiant Heat Exchange

It is concluded from the previous analysis for nude sedentary subjects at thermal equilibrium for very low air ventilation rates that the sense of equal comfort is governed by the constancy of skin temperature and wetness. This basic principle of human comfort can be extended to an environment with different air velocities and with radiant heat exchange. To show the effect of increased air velocity and radiant exchange between the human body and the surroundings, one PTI line was placed in three locations on the psychrometric chart, as shown in Fig. 12. The solid line represents the comfort state for the general population ( $T_s = 85$ ,  $x = .134$ , or  $PTI = -3.5$ ) for very low air ventilation rate and no radiation exchange. The broken line represents the same sense of comfort (same  $x$  and  $T_s$ ) as the solid but with radiant heat loss from the body surface to the surroundings. The dotted broken line represents the same sense of comfort as the other two lines but with high air velocity and no radiation effects. Because the heat and mass transfer coef-

# ENVIRONMENTAL EFFECTS ON NATURAL MOTION LIMIT PTI LINE LOCATIONS

- NATURAL MOTION LIMIT
- RADIANTLY COUPLED
- INCREASED VENTILATION RATE

FIGURE 12

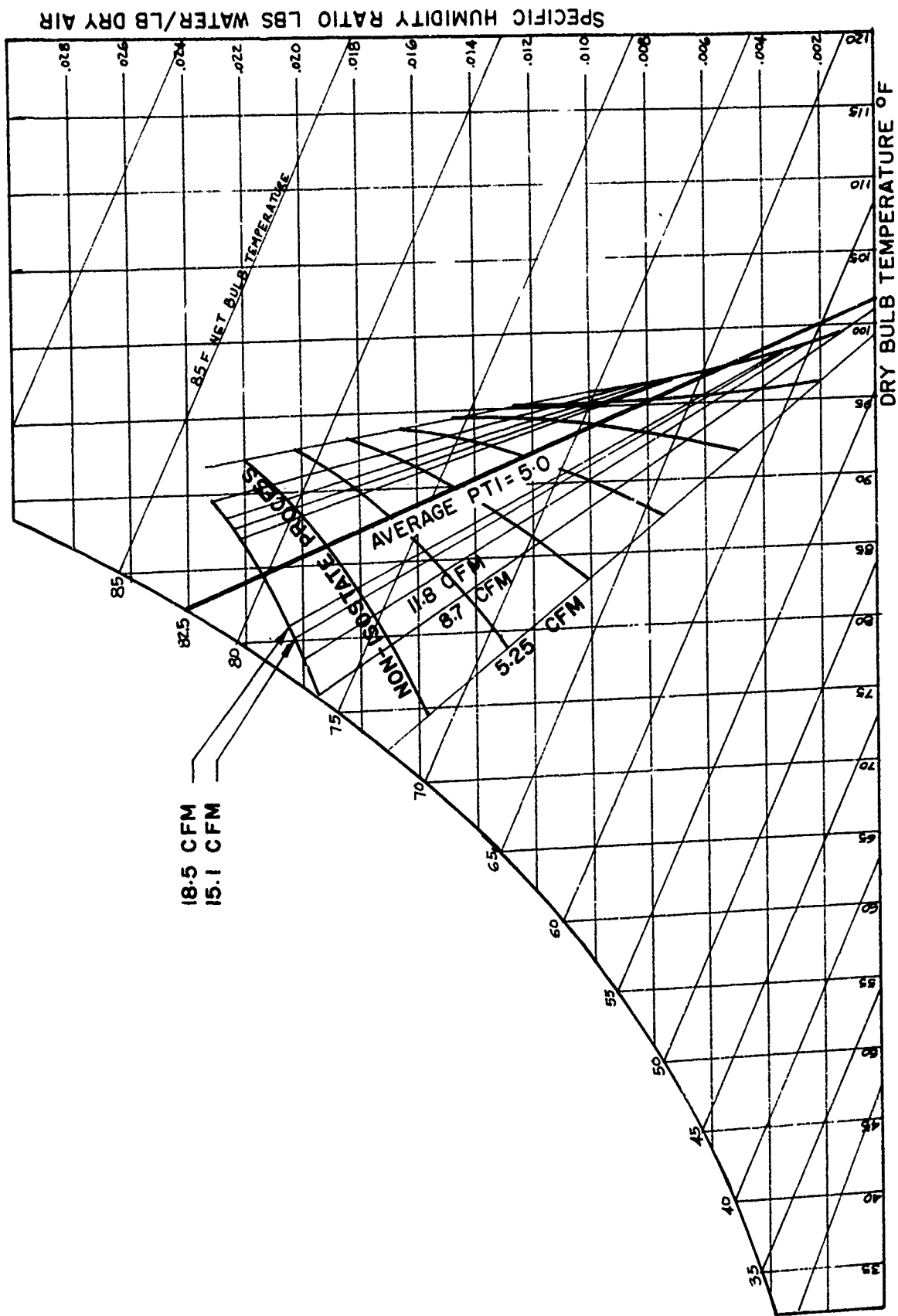




ficients are dependent upon the same parameters, by increasing the air velocity and the heat and mass transfer coefficients will increase but the ratio between them will remain constant. It is noticed from Fig. 12 that by increasing the air velocity the same comfort state must move to a higher environmental condition but the line of comfort of high air velocity is parallel to the one with low air velocity. With the presence of radiation loss the comfort line moves to a higher environment but with steeper slope than that without radiation. This is because the ratio of sensible heat to metabolic heat output is changed with the presence of radiation. From the present analysis it is evident that the human body at any state of comfort or discomfort can be represented by a single point on the  $(x - T_g)$  relation while this same comfort state will be placed differently on the psychrometric chart depending on the heat and evaporative transfer mechanisms and air velocity.

#### Non-isostate Process Lines

The environmental conditions under study are for very low air flow rates and confined space. The air flow rates range from approximately 5 to 20 cfm, which give negligible mechanically induced air velocities in the range of 1 to 2 ft/min. The average PTI line will vary with variation in the air flow rate while keeping the inlet conditions constant. To maintain the same average PTI line the air state at the inlet condition should be changed with change in air flow rate. Figures 13 and 14 show the non-isostate process lines for the average PTI lines equivalent to ET values of 70 and 82.5°F, respectively. The non-isostate line represents loci of inlet and exit states for different air



NON-ISOSTATE PROCESS LINES VERSUS CFM FOR CONSTANT AVERAGE PTI OF 5.0  
(GENERAL POPULATION)

FIGURE 13

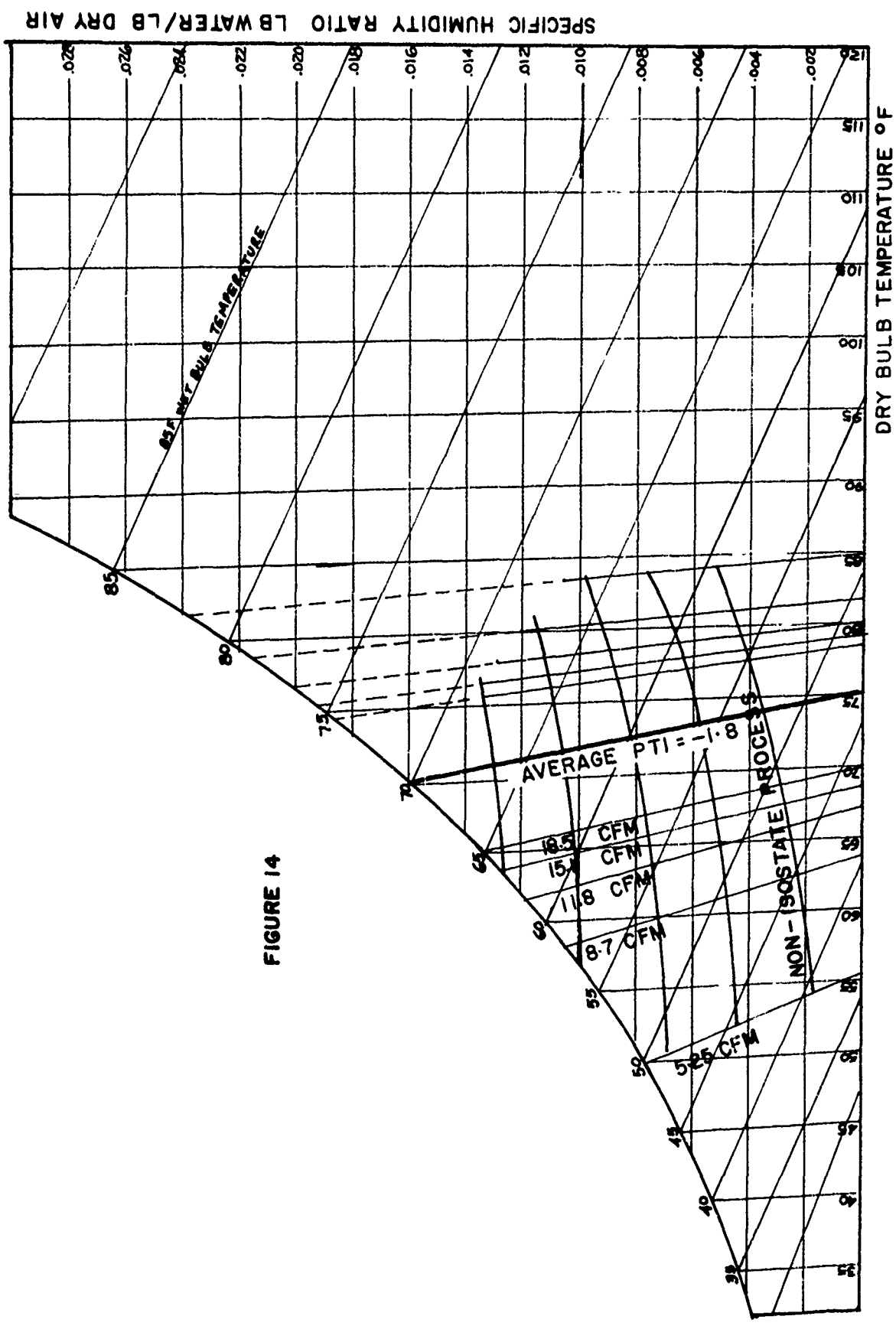


FIGURE 14

NON-ISOSTATE PROCESS LINES VERSUS CFM FOR CONSTANT AVERAGE PTI OF -1.8  
(GENERAL POPULATION)

DRY BULB TEMPERATURE OF

SPECIFIC HUMIDITY RATIO LB WATER/LB DRY AIR

flow rates that would give the same average physiological thermal index. It is noted in Fig. 13 that the exit states asymptotically approach the 95°F dry bulb temperature which represents the skin temperature at the average PTI value of (82.5°F ET).

## V. RESPONSE TO A TRANSIENT THERMAL FLUX

### Review of Literature Predictive Models

One of the objectives of the present study is the development of a predictive thermal model of a human being in a shelter environment upon exposure to transient thermal radiation which simulates the radiation emitted by a ceiling with fire above it.

Two models from the literature that are significant relative to this program objective are those of Machle and Hatch [23] and Kerslake and Waddell [24].

The Machle and Hatch model was developed beginning with a basic energy balance equation similar to Eq. (1) of this report (see Section II)

$$MR - S = E + R + C + W$$

This equation was then expanded as follows:

$$MR' - S = K_r A (T_s - T_w) + K_c A (T_s - T_a) + K_e A X (VP_s - VP_a)$$

where

$$MR' = MR - W \text{ (metabolic rate - work output)}$$

$$A = \text{body surface area}$$

$$T_s = \text{average skin temperature}$$

$$T_w = \text{mean radiant temperature of surroundings}$$

$$T_a = \text{air temperature}$$

$$VP_s = \text{vapor pressure of water at temperature } T_s$$

$$VP_a = \text{vapor pressure of moisture in the air}$$

$$(\text{= \% RH} \times VP @ T_a)$$

$$X = \text{evaporative area/body area}$$

$$K_r, K_c, \text{ and } K_e = \text{coefficients of heat exchange by radiation, convection and evaporation}$$

The storage term,  $S$ , was then expanded to

$$S = cm \left( a \frac{dT_r}{d\tau} + b \frac{dT_s}{d\tau} \right)$$

where

$c$  = average body specific heat

$m$  = body weight

$\frac{dT_r}{d\tau}, \frac{dT_s}{d\tau}$  = rates of change of average values for rectal temperature and skin temperature, respectively.

$a, b$  = weighing factors to proportion the body heat storage relative to the deep body and skin tissues

Also, Machle and Hatch interlocked  $T_s$  and  $T_r$  with the relationship

$$T_r = \eta_0 + \eta_1 T_s$$

or

$$dT_r = \eta_1 dT_s$$

where  $\eta_0, \eta_1$  are constants determined from experimental data.

They were then able to solve for the percentage of equilibrium versus time. The resulting equation is

$$\frac{T_{eq} - T_s}{T_{eq} - T_0} = \exp \left[ - \frac{AC'\tau}{c MR'(a\eta_1 + b)} \right]$$

where

$$C' = K_r + K_c + 2.5 K_e$$

$T_{eq}$  = new equilibrium skin temperature

$T_0$  = initial skin temperature

In this solution it was assumed that  $M, K_r, T_w, K_c, T_a, K_e, X$ , and  $VP_a$  were constant for any given situation.

Upon examination of this equation it can be seen that the time required to reach a given percentage of the new equilibrium is independent of both the surrounding air temperature and the humidity. As will be shown later this is not believed to be factual; the response time is dependent upon surrounding air temperature and humidity.

Another problem with this model is that the rectal and skin temperatures are locked into a direct functional relationship independent of any other parameters. This can be seen as a basic weakness except for very slow changes in environment. This is so, for the skin tissues have only a small thermal capacitance hence they can respond abruptly to changes in environmentally produced heat fluxes and may even go higher than the rectal temperature for a short period of the transient response time. As explained later the predictive model to be proposed gets around this difficulty.

Although there are some inadequacies in the Machle and Hatch model it still has some good points. It appears to be a satisfactory model in the region where there is no active sweating, as well as in the region where the skin is completely wet. The model might have been expanded to include the active sweat region with some follow on work.

Machle and Hatch realized in their study that an environment which would produce the same skin temperature as a second environment could be considered equivalent to the second environment. They were handicapped, however, by not knowing the parameters which influence the variation of skin wetness.

Kerslake and Waddell used the same model as Machle and Hatch with slightly different constants. They investigated the validity of the model when the skin was completely wet. They came to the conclusion that the Machle and Hatch equations were supported by their experimental results.

#### Discussion of the Transient Thermal Flux

In the present work, a predictive technique is desired for a radiant thermal flux which simulates a building fire on the floor above the ceiling of a survival shelter. The literature [25] provides evidence of the time variation and intensity of such radiation fluxes. Several buildings were burned after being instrumented from which contrasting pulses were obtained.

The radiation mode chosen for the present study was that of a library which was shown to have the highest magnitude of radiation flux of any of the buildings burned. The air temperature and humidity were assumed to remain constant during the radiation pulse. Actually, the air temperature and humidity would probably not stay constant. However, to obtain a reasonable basis for comparison between the predictive model and experimental evidence this is assumed so. If there is good agreement between prediction and experiment, no great difficulty is anticipated in dealing subsequently with transient air temperatures and humidities.

#### Predictive Model Problem Statement, Assumption, and Thermal Circuit Schematic

The problem then is to predict the transient thermal behavior of a human subject in terms of skin and deep body temperature

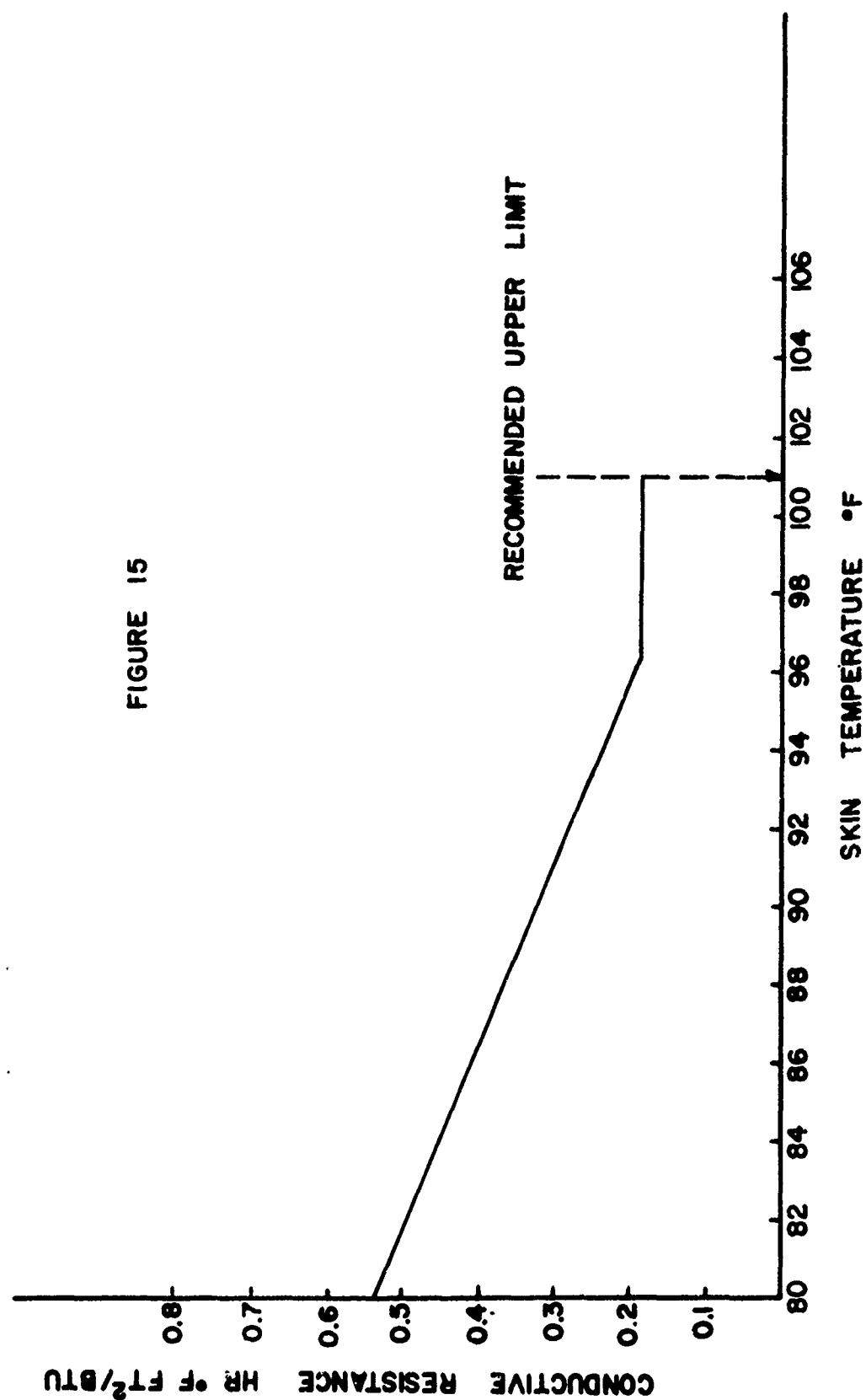


to a thermal radiation flux characterized by a library fire on the floor above the survival shelter.

The assumptions are:

- (a) The sedentary subject is in thermal equilibrium with his environment prior to the pulse.
- (b) He maintains his metabolic output at a constant level.
- (c) The surrounding air temperature and humidity remain constant.
- (d) The relationship of  $(x - T_s)$  developed for equilibrium conditions pertains. This appears justified by the fact that the response of the sweat glands to change in skin temperature is very fast compared to the response of the core and skin temperatures to the proposed change in the thermal environment.
- (e) The apparent thermal conductivity between the skin and the body core is related to the skin temperature as reported by Winslow, et al. [21]. In their study, the reciprocal to the conductivity, the conductive resistance to heat flow, was used. Using their data, Fig. 15 was constructed.

APPARENT BODY CONDUCTIVE RESISTANCE  
VS.  
SKIN TEMPERATURE



The thermal circuit representing the subject exposed to the proposed transient thermal environment is shown in Fig. 16.

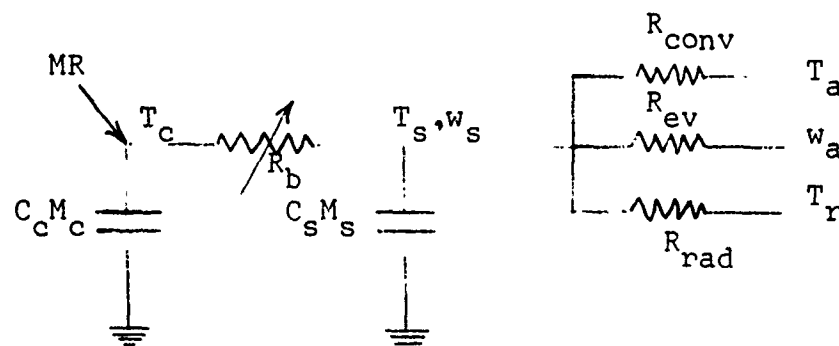


FIGURE 16

$MR$  = (Btu/hr) metabolic rate

$T_s$  = ( $^{\circ}F$ ) average skin temperature

$T_c$  = ( $^{\circ}F$ ) average body core temperature--taken as a weighted mean of rectal and skin temperature [7]

$$T_c = \frac{2}{3} T_r + \frac{1}{3} T_s$$

$T_{a,r}$  = ( $^{\circ}F$ ) temperature of air and radiation source, respectively

$C_c M_c$  = (Btu/ $^{\circ}F$ ) thermal storage capacitance of body tissues

$C_s M_s$  = (Btu/ $^{\circ}F$ ) thermal storage capacitance of skin tissues

$R_b$  = ( $^{\circ}F$  hr/Btu) variable thermal resistance between body core and skin (see Fig. 15)

$R_{conv}$  = ( $^{\circ}F$  hr/Btu) convective heat transfer resistance between skin and surrounding air

$R_{ev}$  = (lbwv/lbda hr/Btu) convective mass transfer resistance between skin and surrounding air

$R_{rad}$  = ( $^{\circ}F$  hr/Btu) radiant heat transfer resistance between skin and surrounding air

$w_{s,a}$  = (Lbwv/lbda) specific humidity of skin and air, respectively.

Referring to Fig. 16, the metabolic output (MR) appears as an energy source within the core of the body. It can either flow out through the skin or be stored in the body resulting in a rise in body temperatures. The resistance,  $R_b$ , is shown as variable as it includes the effect of vasodilation of the peripheral blood vessels with skin temperature increase.

The thermal capacitors represent the body energy storage components. The core capacitance represents 97% of the storage capability and the skin tissues are assigned 3%. These percentages are admittedly assigned somewhat arbitrarily for want of complete understanding. The three resistors between the skin and the environment represent the heat flow impedances due to evaporation, convective heat transfer, and radiation. The radiation resistance is shown as variable to picturize the transient thermal radiation pulse.

#### Derivation of Thermal Response Equations

By consideration of energy rates at the nodel points,  $T_c$  and  $T_s$ , the following equations result.

For the node at  $T_c$

$$MR - C_c M_c \frac{dT_c}{d\tau} - \frac{(T_c - T_s)}{R} = 0 \quad (26)$$

For the node at  $T_s$

$$\frac{T_c - T_s}{R_b} - C_s M_s \frac{dT_s}{d\tau} \left[ \frac{T_s - T_a}{R_{conv}} + \frac{w_s - w_a}{R_{ev}} + \frac{T_s - T_r}{R_{rad}} \right] = 0 \quad (27)$$

These can be rearranged

$$C_c M_c \frac{dT_c}{d\tau} = MR - \frac{(T_c - T_s)}{R_b} \quad (28)$$

$$C_s M_s \frac{dT_s}{d\tau} = \frac{T_c - T_s}{R_b} - \left[ \frac{T_s - T_a}{R_{conv}} + \frac{w_s - w_a}{R_{ev}} + \frac{T_s - T_r}{R_{rad}} \right] \quad (29)$$

### Method of Solution

Working with Eqs. (28) and (29) a digital computer solution was easily obtained by using a Runge-Kutta method for solving two differential equations simultaneously. The independent variable was time,  $\tau$ . The dependent variables were the skin temperature,  $T_s$ , and the core temperature,  $T_c$ . The initial conditions were:  $\tau = 0$ ,  $T_s = 95.3^\circ\text{F}$ ,  $T_c = 98.1^\circ\text{F}$ . Parametric values were:  $MR = 400 \text{ Btu/hr}$ ; body surface area =  $20 \text{ ft}^2$ ; body mass =  $160 \text{ lbm}$ ; body thermal capacitance =  $0.83 \text{ Btu/lbm}^\circ\text{F}$ ;  $h_c$  and  $h_m$  were natural motion limit values;  $h_c = .76 \text{ Btu/hr ft}^2^\circ\text{F}$ ,  $h_m = 1.4 \text{ lbm wv/hr ft}^2$  ( $\text{lbm wv/lbm da}$ );  $T_a = 92^\circ\text{F}$ ,  $w_a = 0.0129 \text{ lbm wv/lbm da}$  (note: this is an  $82^\circ\text{F ET}$ ).

It should be noted that the initial skin temperature is such that the occupant is actively sweating at the onset of the radiant pulse.

### Interpretation of Results

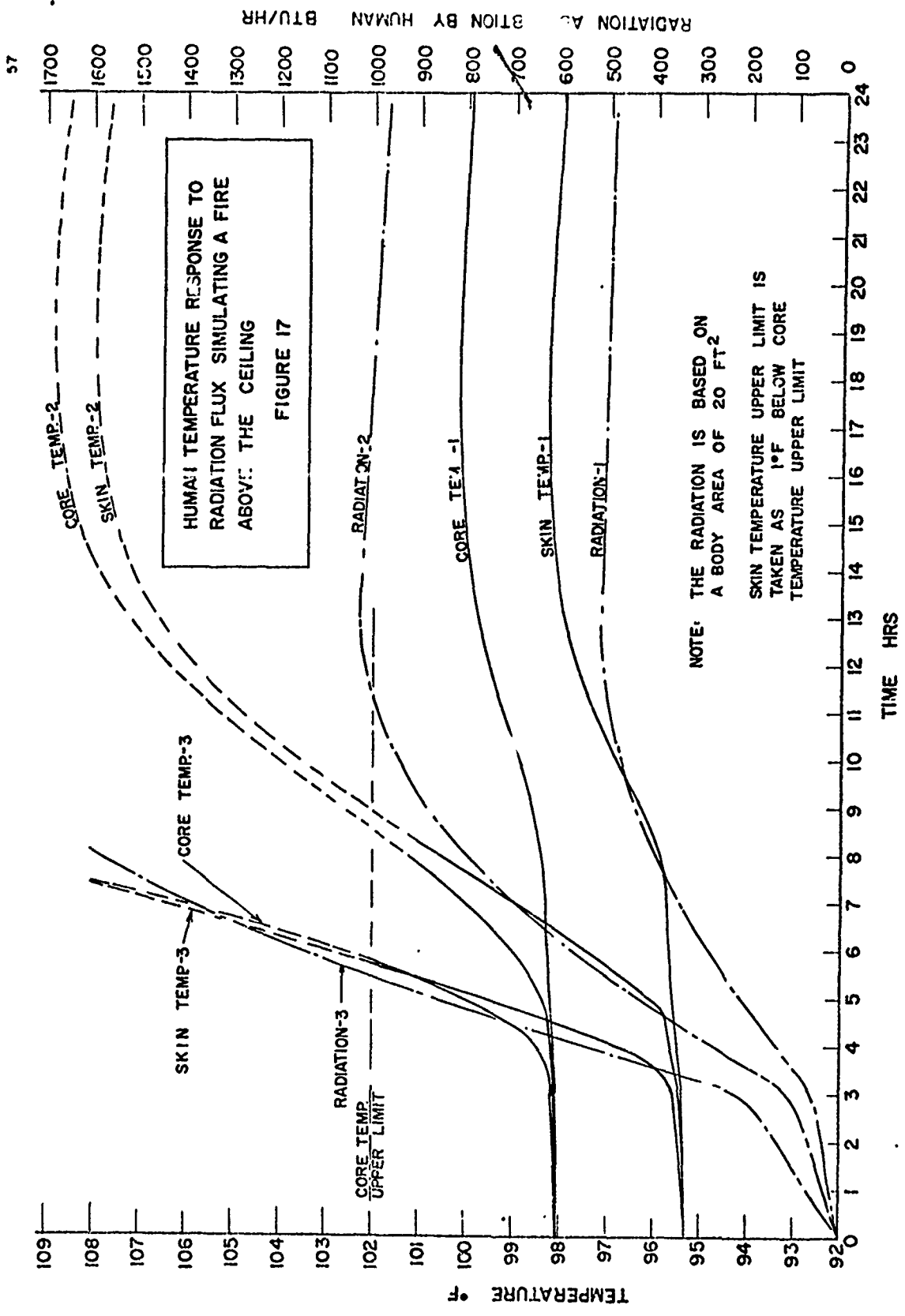
The results obtained from this analytical model are shown in Fig. 17. The radiation fluxes were taken as percentages of curve 70-6, Fig. 5, Ref. [25].

Radiation - 1 = 25% of the heat flux from the ceiling is (see Fig. 17) intercepted as heat flux by the occupant.

Radiation - 2 = double Radiation - 1 (i.e., 50% of the flux is intercepted).

Radiation - 3 = double Radiation - 2 (i.e., 100% of the flux is intercepted).

Consider the graphical results for Radiation - 1. It is evident that the occupant can maintain thermoregulatory control for approximately eight hours after the onset of the radiant pulse (see skin temperature - 1 and core temperature - 1 of Fig. 17). After eight hours there is a loss of thermoregulatory



57

control but the skin and core temperatures do not exceed the survival limit which is taken as a body core temperature of  $102^{\circ}\text{F}$ .

Referring to Radiation - 2 results it is seen that the person loses control of his core and skin temperature after about five hours. The person would definitely not make it through the fire and would reach a point beyond the core temperature limit in eight and one-half hours.

Referring to Radiation - 3 the limit would be reached in less than six hours.

There are two very important points to be made in addition to the evidence shown in Fig. 17. First, the body temperature response of the shelter occupant will be strikingly different to the radiation pulse depending upon whether the occupant was initially in a passive moisture loss condition, an active sweating condition as displayed in Fig. 17, or near the total sweating condition ( $x = 1$ ). Computer runs have revealed these contrasts. They are not reported here as experimental corroboration of the predictive evidence should be achieved before presenting such details.

The second point has also been seen from this computer model although it is not shown on the graph. That is, if the humidity is lowered while keeping the same effective temperature, the response of the skin and core will be relatively slower from the same radiation pulse. This can be seen by referring to Eq. (29). When  $w_a$  is lower the effect of changing the skin wetness will have a greater effect on controlling the skin temperature by evaporation. Since the skin wetness is directly proportional to the skin temperature in the active sweat region, this will slow down

the skin temperature rise compared to the higher humidity point at the same effective temperature. This result is inconsistent with the model by Machle and Hatch which predicts that the lowered humidity should have no effect on the time it takes to reach equilibrium.

A further note of emphasis on the response of the body in the active sweat region is that the cooling power of the sweat glands keeps the skin and core temperatures almost constant over a wide range of conditions. If the body is already heated to a point where the subject actively sweats and then the environment is changed to a new point which is still in the active sweat region, he will reach equilibrium very quickly as his sweat glands provide the primary response. The skin and core temperatures will change only slightly in reacting to the new environment.



## VI. SUMMARY, CONCLUSION AND RECOMMENDATIONS FOR FOLLOW-ON ACTIVITIES

### Project Summary and Conclusions

The program objectives were to establish a physical basis for the prediction of environmental states which would appear as equally comfortable or uncomfortable to the human being. Particular attention was to be given to environments with very low air circulation rates. The results from the predictive technique were then to be compared with past and current experimental evidence obtained from the monoman calorimeter. The results were also to be compared with evidence found in the literature. In addition to this main program, and predicated on a reasonably successful derivation of a predictive model, an extension of the predictive model was to be attempted. This extension would consider the effect on the human subject of a transient (i.e., several hours) radiation flux. The flux would simulate the effects of a building fire on the floor above a shelter space. The effect on the test subject would be predicted in terms of skin and body core time-temperature relationships.

The following summary relates to these program objectives and is generated from the previous sections of this report:

(1) The relationship of the percentage of the body's sweat glands that are activated ( $x$ ) to the body's skin temperature ( $T_s$ ) has been established from experimental evidence for sedentary persons. It has three distinct regions: the passive moisture loss region, the active sweating region, and the region wherein the thermoregulatory function is lost. This relationship is the resultant of both the internal body thermoregulatory processes and the external stress caused by the environment.

The ( $x - T_s$ ) relation is the physical index that is identifiable at the skin surface which defines thermal comfort for sedentary subjects. Values on this ( $x - T_s$ ) curve are identified as Physiological Thermal Index values. Thermal comfort zones are also identified on this relationship. Two notes of caution; first, the need must be recognized for more extensive testing of subjects especially in the region of lost thermoregulatory function and in the transitions between the three regions. Second, the relationship applies only to sedentary persons. Whether and how much it will be modified for other activity levels is also subject to further experimentation.

(2) From the energy balance and transport rate equations coupling the subject's skin surface state and the surrounding environment, and incorporating the ( $x - T_s$ ) relationship, air states of equal comfort (PTI constant lines) can be established on the psychrometric chart. A PTI constant line will appear at different locations on the chart depending upon air flow rates, metabolic rate per unit of body area, amount of clothing, and the presence of thermal radiation. The relocation of these lines is easily accomplished by variation of computer program parameters. Hence, comfort zones and PTI constant lines can be established on the psychrometric chart for any mix of these conditions.

(3) The PTI constant lines are in reasonable agreement with the effective temperature lines established by Yaglou in the 82 to 85°F ET range. At lower ET values, the ET lines overestimate humidity effects in comparison with the PTI constant

lines. Experimental evidence from the monoman calorimeter and the work of other investigators support the view that the PTI lines are a better representation of constant comfort states than are the ET lines in this region. For ET values greater than 85°F there is agreement with other experimentors that in this region the ET lines are an underestimation of the humidity effect. The PTI lines again agree better with monoman calorimeter evidence and with the other experimental evidence.

(4) The modified predictive model which incorporates the  $(x - T_s)$  relationship and body thermal capacitance and resistance effects appears useful in handling transient thermal radiation pulses that are associated with fires adjacent to shelter areas. A distinctly different body time-temperature response is observed depending upon which of the three regions of the  $(x - T_s)$  relationship are involved during the transient response. It is evident from these results that countermeasures for dealing with these thermal pulses must take into account the initial thermal environmental conditions for the human's tolerance for the same radiation pulse will vary seriously depending upon these initial conditions.

The results generated from the transient predictive model have not been corroborated by experimental test work in the calorimeter.

#### Recommendations for Follow-on Activities

There are several areas of meaningful extension of the existing program activities. They can best be indicated by asking the following questions:

- (1) What are the true natures of the transitional segments of the  $(x - T_s)$  relationship between its three distinct regions?
- (2) Are the natural motion limiting values of the convective heat and mass transfer coefficients fully established?
- (3) Does the  $(x - T_s)$  relationship pertain to activity levels other than sedentary and if not how does it modulate?
- (4) Does a human respond as predicted when exposed to transient thermal radiation fluxes?

There are many other questions that can be raised. However, it is believed by the authors that the aforementioned ones are the most meaningful that can be answered for the least cost and modification of the existing project facilities.

## APPENDIX 1

### SKIN TEMPERATURE APPARATUS

In the earlier stages of experimental work on this project, a two point skin temperature harness was developed. Elastic metallic bands were used to hold thermocouples in contact with the skin tissues yet allow evaporative and convective heat transfer. Because the early tests were at high effective temperatures, the skin tissue temperatures were nearly uniform and it was subsequently shown [26] that the two point harness provided a satisfactory average value of the skin temperature,  $T_s$ .

Since that time, environmental test conditions have been cooler and less humid which resulted in greater skin temperature variation and a requirement for more measuring points. The decision was made to use the same system of attachment and measurement as before and expand the number of skin measuring points to twelve. The twelve points were the forehead, cheek, upper arm, forearm, hand, thigh, calf, foot, and four points on the trunk. The average skin temperature is found by multiplying the temperature at each particular point by the percentage of body surface area that particular point represents (see Ref.[27] for surface area distribution). For instance, the calf temperature reading would be multiplied by 0.13 since the calf accounts for 13% of the skin's surface area. After a careful evaluation study [26], the twelve point harness was used for the majority of the tests herein reported.

Problems with this expanded system began showing up almost immediately. The number of wires, straps, and bands cluttered the desk at which the test subject sits, and by their very

awkwardness and limited freedom precluded any attempts to prevent their tangling. The thermocouple wires broke frequently as a result and the test subjects complained of the limited mobility [16].

As a result, the Mechanical Engineering Department purchased a telemetry device--transmitter, stepping switch and batteries which is small enough (2" x 1" x 3") to be worn as a waist pack, and a receiver. The sensors are thermistors. The thermistors were incorporated in nylon net bands that used velcro tape for size adjustment and attachment to the sites on the test subject's body. This was a considerable improvement over the metallic elastic band type of attachment previously used.

The receiver outside the calorimeter easily monitors the transmitted signal and displays the skin temperature readings to the nearest °C. A frequency counter permits determination of the temperature to the nearest 0.1°C. The stepping switch steps the transmitted signal every 30 seconds. There are nine points incorporated in this skin temperature measuring harness.

Thus,  $T_s$  is taken in our experiments using this system as the weighted average of nine observations at different points on the body surface and calculated as follows [16]:

$$\begin{aligned} T_s = & .19 T_{thi} + .14 T_{arm} + .035 T_{chk} + .035 T_{head} \\ & + .05 T_{hand} + .07 T_{feet} + .13 T_{clf} + .175 T_{stch} \\ & + .175 T_{back}; \end{aligned}$$

where the readings of skin temperatures are time averaged for the different parts of the body.

Initial comparisons between the new portable skin temperature harness and the thermocouple harness revealed a systematic discrepancy. This was traced to an incorrect calibration curve supplied by the manufacturer of the telemetry equipment. Upon correcting the calibration, satisfactory comparisons were made. To date, the telemetry system has proven far superior in dependability and comfort to the wearer.

## APPENDIX 2

### LOGARITHMIC MEAN AVERAGE

In the monoman calorimeter, the air temperature and humidity changes as the air flows along the human body length, see Fig. 1.

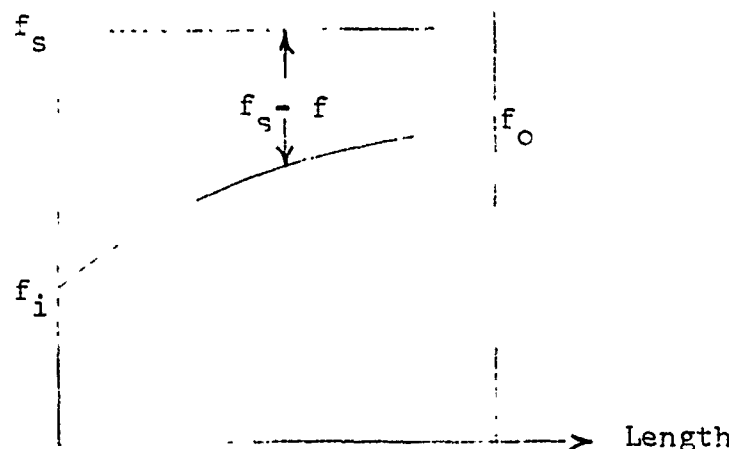


FIG. 1: PROPERTY PROFILE OF AIR AS IT PASSES ALONG THE BODY LENGTH AT CONSTANT PROPERTY  $f_s$

For simplicity, it is considered that under equilibrium conditions, skin temperature of the human body remains uniform and constant at  $T_s$ . The skin surface heat and mass transfer rate equations are of the form

$$\dot{P} = h_p A_{tr} (f_s - f) \quad (1)$$

where

$\dot{P}$  = rate of transfer of quantity P per unit time

$A_{tr}$  = surface area from which the transfer occurs

$f$  = property equilibrium index

$f_s - f$  = property difference which is the driving force causing transfer of P, property at skin surface minus average property of the surrounding environment

$h_p$  = average convective transfer coefficient for P per unit time, unit area, and unit property difference causing the transfer



Also from the steady flow energy equation the rate of transfer of quantity P can be written as

$$P = G \lambda_p (f_o - f_i) \quad (2)$$

where

$G$  = fluid mass flow rate lbm/hr

$\lambda_p$  = specific quantity, rate of transfer of quantity P  
per unit mass flow rate per unit property difference.

For the element of length  $dx$  with associated quantity transfer area  $dA_{tr}$

$$\dot{dP} = h_p (f_s - f) dA_{tr} \quad (3)$$

Also for the property change  $df$  associated with quantity rate transfer  $\dot{dP}$

$$\dot{dP} = G \lambda_p df \quad (4)$$

From Eqs. (3) and (4)

$$df = \frac{\dot{dP}}{G \lambda_p} = \frac{h_p (f_s - f)}{G \lambda_p} dA_{tr} \quad (5)$$

or

$$\frac{df}{(f_s - f)} = \frac{h_p}{G \lambda_p} dA_{tr}$$

Integrating both sides over the whole body length with associated transfer area  $A_{tr}$  and change of property from  $f_i$  to  $f_o$

$$\ln \frac{f_s - f_i}{f_s - f_o} = \frac{h_p A_{tr}}{G \lambda_p}$$

Substituting Eq. (2) into the above equation

$$\ln \frac{f_s - f_i}{f_s - f_o} = \frac{h_p A_{tr} (f_o - f_i)}{P}$$

or

$$\dot{P} = h_p A_{tr} \frac{f_o - f_i}{\ln \left( \frac{f_s - f_i}{f_s - f_o} \right)} \quad (6)$$

By comparing Eqs. (1) and (6)

$$(f_s - f_a) = \frac{f_o - f_i}{\ln \frac{f_s - f_i}{f_s - f_o}}$$

or

$$f_a = f_s - \frac{f_o - f_i}{\ln \left( \frac{f_s - f_i}{f_s - f_o} \right)} \quad (7)$$

where  $f_a$  is the logarithmic mean property value.

In the case of convective heat transfer, the property  $f_a$  is the temperature and Eq. (7) becomes

$$T_a = T_s - \frac{T_o - T_i}{\ln \left( \frac{T_s - T_i}{T_s - T_o} \right)} \quad (8)$$

and in the case of mass transfer, the property  $f$  is the specific humidity;  $w$ , and Eq. (7), become

$$w_a = w_s - \frac{w_o - w_i}{\ln \left( \frac{w_s - w_i}{w_s - w_o} \right)} \quad (9)$$

## APPENDIX 3

This program computes average air states, sensible and evaporative heat outputs, inlet and exit air states that correspond to constant skin temperature and constant wetness under different air flow rates. The  $(x - T_s)$  relation, shown in Fig. 3 of the body of this thesis, is simplified and represented by three straight line equations representing the three distinct regions of the  $(x - T_s)$  curve. The three straight line equations are incorporated in the program. The metabolic rate and body surface area may be varied as program parameters but are taken here for the average adult male.

Symbols Used in the Program\*

LH	evaporative heat output rate, Btu/hr
WI	air humidity ratio at inlet state, lbs water vapor/lb dry air
HM	convective mass transfer coefficient (determined in Chapter II, lbm water vapor/hr ft <sup>2</sup> (lbm water vapor/lbm dry air)
HFG	latent heat of vaporization of one pound of water, Btu/hr
A	body surface area, ft <sup>2</sup>
PVS	water vapor pressure at skin temperature, lbs per square feet
WS	humidity ratio that corresponds to saturated air at $T_s$ , lbs water vapor/lb dry air
CP	specific heat of dry air at normal temperatures, Btu/(lb)(°F)
HC	convective heat transfer coefficient, Btu/hr/sq ft/°F
G	mass flow rate, lbm/hr
WO	air humidity ratio at exit state, lbs water vapor/lb dry air
SH	sensible heat output rate, Btu/hr
TI	inlet air dry bulb temperature, °F
TO	exit air dry bulb temperature, °F
TA	logarithmic mean average of air dry bulb temperature, °F

---

\* Symbols not listed above are defined within the program itself.

WA logarithmic mean average of air humidity ratio, lbm water vapor/lbm dry air  
 RW water vapor gas constant, ft lbf/(lbm)(°F)  
 RA dry air gas constant, ft lbf/(lbm)(°F)  
 P atmospheric pressure, lbf/ft<sup>2</sup>  
 QI air flow rate at inlet state, ft<sup>3</sup>/hr  
 X fraction of skin surface that is wet

# Program Statements

```

SUBROUTINE GWILP (X,TS)
REAL LH
DO 13 I=1,301,25
WI=I/10000.
HM=1.4
C LATENT HEAT OF VAPORIZATION IS TAKEN AT SATURATED WATER
  TEMPERATURE OF 95°F
HFG=1039
A=20.0
PVS=3.61*TS-225.
WS=(.622*PVS)/(2116.-PVS)
CP=0.24
HC=.765
G=51.4
Z=HM*A*X/G
WO=WS-(WS-WI)*EXP(-Z)
B=ALOG((WS-WI)/(WS-WO))
LH=HM*A*X*HFG*(WO-WI)/B
SH=400.-LH
Y=(HC*A)/(G*CP)
TI=TS-SH/(G*CP*(1.-EXP(-Y)))
TO=TI+SH/(G*CP)
E=ALOG((TS-TI)/(TS-TO))
TA=TS-(TO-TI)/E
WA=WS-(WO-WI)/B
DO15IG=25,85,15
G=IG
Y=(HC*A)/(G*CP)
Z=HM*A*X/G
TI=TS-SH/(G*CP*(1.-EXP(-Y)))
TO=TI+SH/(G*CP)
WI=WS-LH/(G*HFG*(1.-EXP(-Z)))
WO=WI+LH/(G*HFG)
RW=1544./18.02
RA=1544./29.95
P=14.7*144.
QI=((TI+460.)*G/P) ((WI*RW+RA)/(1.+WI))
WRITE(5,9)X,TS,TI,TO,WI,WO,TA,WA,SH,LH,QI,G
9 FORMAT (12 F10.4)
15 CONTINUE
WRITE(5,11)

```

```
11  FORMAT(1)
13  CONTINUE
    WRITE(5,14)
14  FORMAT(11)
    RETURN
    END
    C  THE FOLLOWING IS THE MAIN PROGRAM
    WRITE(5,12)
12  FORMAT(9X,'X',8X,'TI',8X,'TO',8X,'WI',8X,'WO',8X,'TA',8X,
      'WA',8X,'SH',8X,'LH',8X,'QI')
    DO 10 ITS=85,95
      TS=ITS
      X=(.00234+.00271*TS)/1.4
      CALL GWILP(X,TS)
10  CONTINUE
      DO 16 IHMX=3,14
        X=(IHMX*.1)/1.4
        TS=94.87355+.64431*(IHMX*.1)
        CALL GWILP(X,TS)
16  CONTINUE
      DO 17 JTS=96,100,1
        TS=JTS
        X=1
        CALL GWILP(X,TS)
17  CONTINUE
      CALL EXIT
    END
```

## REFERENCES

1. Monoman Calorimeter Project, Final Report for Office of Civil Defense by R. K. Pefley, E. T. Cull and K. M. Sekins, January 1969.
2. "Determining Lines of Equal Comfort", by F. C. Haughton and C. P. Yaglou, ASHVE Trans., 29:163, 1923.
3. "Comfort Reactions of 275 Workers During Occupancy of Air Conditioned Spaces", by F. B. Rowley, R. C. Jordan and W. E. Snyder.
4. "A Method for Improving the Effective Temperature Index", by C. P. Yaglou, ASHVE Trans., 53:307, 1947.
5. "Difference Between Men and Women in Their Response to Heat and Cold", by J. D. Hardy and E. F. DuBois. Proceedings of National Academy of Sciences, 26:389, June 1940.
6. See Reference 4.
7. "Physiological Reactions of the Human Body to Varying Environmental Temperatures", by E. A. Winslow, L. P. Herrington and A. P. Gagge, The American Journal of Physiology, Vol. 120, Sept. 1, 1937.
8. "Free Convection Coefficients of Heat and Mass Transfer from a Human Being in a Warm, Humid, Still Air Environment", T. H. Miyashiro, M.S. Thesis, University of Santa Clara, 1967.
9. "Thermal Exchanges of Man at High Temperatures", by N. Nelson, L. W. Eichna, S. M. Horvath, W. B. Shelley and T. F. Hatch, American Journal of Physiology, Vol. 151; 626, 1947.
10. Human Physiology, by B. A. Housay, et al., McGraw-Hill Book Company, New York, 1951, p. 375.
11. "Physiological Reactions of the Human Body to Various Atmospheric Humidities", by C. E. Winslow, L. P. Herrington, and A. P. Gagge, American Journal of Physiology, Vol. 120, No. 2, Oct. 1937.
12. United States Census of Population, 1960, U.S. Department of Commerce, Bureau of Census, Washington, D.C.
13. ASHRAE Handbook of Fundamentals, ASHRAE, Inc., New York, 1967, p. 114, Fig. 2, and p. 119, Table 3.
14. "An Effective Temperature Scale Based on a Simple Model of Human Physiological Regulatory Response", by A. P. Gagge, J.A.J. Stolwijk, and Y. Nishi, ASHRAE Trans., 1970, Vol. 77, Part I, pp. 247-262.

15. Temperature Regulation in Man--A Theoretical Study, by J.A.J. Stolwijk and J. D. Hardy, Pflüger Archiv, 291:129-162, 1966.
16. "A Practical Approach to Engineering Design Problems in Relation to the Design of a Skin Temperature Harness", B.S. Thesis by Michael L. Dixon, University of Santa Clara, May 1971.
17. "Effective Temperature with Clothing", by C. P. Yaglou and E. Miller, ASHVE Trans., Vol. 31, 89, 1925.
18. ASHRAE 1966.
19. Indices of Comfort, by C. P. Yaglou, Chapter 9, edited by L. H. Newburgh, W. B. Saunder Co., Philadelphia, 1949.
20. "The Prediction of Thermal Comfort when Thermal Equilibrium is Maintained by Sweating", by A. P. Gagge, J.A.J. Stolwijk and Y. Nishi, ASHRAE Trans., Vol. 75, Part II, pp. 108-125, 1969.
21. "Model Skin Temperature--An Index of Thermal Sensation in Cold, Warm and Humid Environments", by Y. Nishi and K. Ibamoto, ASHRAE Trans., Vol. 75, Part II, 1969.
22. "The Nature of Thermal Comfort for Sedentary Man", by F. Rohles and R. Nevins, 1971 ASHRAE Semi-Annual Meeting, Philadelphia, Pa.
23. "Heat - Man's Exchanges and Physiological Responses", by W. Machle and T. F. Hatch, Physiological Review, Vol. 27, pp. 200-227, 1947.
24. "Heat Exchanges of Wet Skin", by D. McK. Kerslake and J. L. Waddell, Journal of Physiology, Vol. 141, pp. 156-163, 1958.
25. Fire Laboratory Tests - Phase II, Final Report, IITRI-J6217(2), IITRI, February 1972.
26. "A Study of Skin Temperature Measurement in the Monoman Calorimeter", B.S. Thesis, Thomas J. Kirn, University of Santa Clara, 1969.
27. "Full Scale Human Body Model Thermal Exchange Compared with Equatorial Condensations of Human Calorimetric Data", Trans. of the ASME, Journal of Heat Transfer, Series C, Vol. 81, Aug. 1959, pp. 187-194.